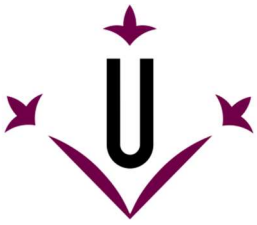

DNA activates the Nse2/Mms21 SUMO E3 ligase in the Smc5/6 complex

Nathalia Varejão[1], Eva Ibars[2], Jara Lascorz[1], Neus Colomina[2], Jordi Torres-Rosell,[2,*] and David Reverter[1,*]

[1]Institut de Biotecnologia i de Biomedicina (IBB) and Dept. de Bioquímica i Biologia Molecular, Universitat Autònoma de Barcelona, 08193 Bellaterra, Spain.
[2]IRBLLEIDA, Dept. Ciències Mèdiques Bàsiques, Universitat de Lleida, Lleida, Spain.

* Correspondence: david.reverter@uab.cat (D.R.), jordi.torres@cmb.udl.cat (J.T.-R.)

SUMMARY

Modification of chromosomal proteins by conjugation to SUMO is a key step to cope with DNA damage and to maintain the integrity of the genome. The recruitment of SUMO E3 ligases to chromatin may represent one layer of control on protein sumoylation. However, we currently do not understand how cells upregulate the activity of E3 ligases on chromatin. Here we show that the Nse2 SUMO E3 in the Smc5/6 complex, a critical player during recombinational DNA repair, is directly stimulated by binding to DNA. Activation of sumoylation requires the electrostatic interaction between DNA and a positively-charged patch in the *ARM* domain of Smc5, which acts as a DNA sensor that subsequently promotes a stimulatory activation of the E3 activity in Nse2. Specific disruption of the interaction between the *ARM* of Smc5 and DNA sensitizes cells to DNA damage, indicating that this mechanism contributes to DNA repair. These results reveal a mechanism to enhance a SUMO E3 ligase activity by direct DNA-binding and to restrict sumoylation in the vicinity of those Smc5/6-Nse2 molecules engaged on DNA.

INTRODUCTION

Genome integrity is under constant surveillance. External insults, the metabolism of the cell and most chromosome transactions can damage the genome, resulting in deleterious mutations or cell death. Cells have therefore developed DNA repair and DNA damage tolerance mechanisms, which often require post-translational modifications to recruit and activate repair factors. Post-translational modification by conjugation to the small ubiquitin-like modifier SUMO actively participates in maintaining the integrity of the genome: SUMO plays pivotal roles during chromosome replication and segregation and in virtually all DNA repair mechanisms (Bergink & Jentsch, 2009). In fact, the extensive sumoylation of many DNA repair and replication factors constitutes an integral part of the DNA damage response (Cremona *et al*, 2012).

SUMOylation involves the formation of an isopeptide bond between the ε-amino group of a lysine residue and the C-terminus of the SUMO protein. This reaction requires the participation of an E1 activating enzyme (Uba2/Aos1) that passes the SUMO proteins to an E2 conjugating enzyme (Ubc9). Once charged with SUMO, Ubc9 transfers SUMO to the target protein. This can occur directly, by recognition of a SUMO consensus motif (Bernier-Villamor *et al*, 2002; Yunus & Lima, 2006), but most often requires the participation of an E3 SUMO ligase enzyme. Budding yeast codes for three mitotic SUMO E3 ligases, including two members of the PIAS family (Siz1 and Siz2) and the Siz/PIAS-related Nse2 protein (Johnson & Gupta, 2001; Zhao & Blobel, 2005). Since the E1 and E2 enzymes in the SUMO pathway lack known DNA binding domains, modification of chromosome-bound proteins seems to rely on recruitment of SUMO E3 ligases to chromatin (Ulrich, 2014). This can occur by direct binding of the E3 ligase to DNA, by interaction of the E3 with chromosome-associated proteins, or by granting access of the E3 to DNA lesions via previous phosphorylation and ubiquitination events at damaged sites. For example, an N-terminal SAP domain localize Siz2 on DNA, where it promotes sumoylation of homologous recombination factors (Psakhye & Jentsch, 2012); additionally, Siz2 binds ssDNA through interaction with the ssDNA binding replication protein A (RPA) (Chung & Zhao, 2015). The Nse2 SUMO ligase, a subunit of the Smc5/6 complex, has also been shown to play key roles in the maintenance of chromosome integrity (Zhao & Blobel, 2005; Ampatzidou *et al*, 2006; Behlke-Steinert *et al*, 2009; Bermúdez-López *et al*, 2015; Branzei *et al*, 2006; Chavez *et al*, 2010; Pebernard *et al*, 2008b; Potts *et al*, 2006). As Nse2 lacks DNA-binding domains, its DNA repair functions require its stable docking onto the Smc5 protein (Duan *et al*, 2009; Bermúdez-López *et al*, 2015), and the subsequent association of the Smc5/6 complex with damaged sites (Bustard *et al*, 2012; Lindroos

et al, 2006; De Piccoli *et al*, 2006; Tapia-Alveal & O'Connell, 2011).

SMC (*Structural Maintenance of Chromosomes*) complexes are topologically closed molecules formed by the heterodimerization of two elongated SMC subunits and by a distinct number of associated non-SMC elements (Uhlmann, 2016). SMC proteins contain three different domains: an ATPase head structurally related to that of *ABC* transporters (hereafter named "*HEAD*"), an extended coiled coil region ("*ARM*") and a heterodimerization or hinge domain ("*HINGE*"). While hinge heterodimerization closes the molecule at one end, a kleisin subunit connects the two ATPase heads at the other end, defining an inner compartment delimited mainly by two long coiled coils. Each SMC complex has specific and essential roles: cohesin maintains connections between sister chromatids, condensin compacts chromosomes and Smc5/6 promotes chromosome disjunction. Despite these seemingly disparate functions, all SMC complexes share a common property, which is to organize chromosomes by topologically embracing DNA inside their ring-shaped structure. This function requires the ATPase activity of the head domains, which regulates the entry and release of DNA fibers inside the SMC ring. In prokaryotes, the ATPase-dependent conformational changes in the head domain can affect the architecture of the coiled coil domains, altering the ability of SMC molecules to embrace DNA (Bürmann *et al*, 2017).

Once loaded onto chromatin, Smc5/6 participates in critical chromosome transactions during DNA replication and repair. The Smc5 and Smc6 subunits can bind strongly to DNA in vitro through several binding regions located in the hinge, the head and the arm regions (Alt *et al*, 2017; Roy & D'Amours, 2011; Roy *et al*, 2011, 2015). In vivo, the affinity of the SMC core for DNA is regulated by the other six non-SMC subunits (Nse proteins). Nse4, the kleisin subunit in the Smc5/6 complex, associates with Nse1 and Nse3 to constitute a stable sub-complex. The Nse1-Nse3 pair contains a patch of positively-charged residues that acts as a DNA-binding surface and mediates Smc5/6 loading onto chromatin (Zabrady *et al*, 2016a). Although no specific function has been attributed to the Nse5 and Nse6 subunits, their alleged functional homologues in vertebrates (SLF1 and SLF2) have been proposed to promote recruitment of the Smc5/6 complex to interstrand cross-links (Räschle *et al*, 2015).

The Nse2 SUMO ligase has an undefined role in sister chromatid recombination and chromosome disjunction by promoting the sumoylation of several targets including subunits in the cohesion (Potts *et al*, 2006; Almedawar *et al*, 2012; McAleenan *et al*, 2012), Smc5/6 (Bermúdez-López *et al*, 2015) and STR complexes (Bermúdez-López *et al*, 2016; Bonner *et al*, 2016). To reach its substrates, the E3 domain must first dock onto the central part of the *ARM* region of Smc5 through a long N-terminal helical domain (Duan *et al*, 2009). While docking of Nse2 onto Smc5 through the N-terminal

domain is essential for viability (Bermúdez-López *et al*, 2015; Duan *et al*, 2009), the C-terminal *RING* domain, which codes for the E3 SUMO ligase activity, is dispensable; however, mutations in the SUMO ligase domain render cells sensitive to DNA damage, highlighting its relevance in genome maintenance.

It is currently unclear if all Smc5/6-Nse2 molecules are SUMO-active, potentially targeting soluble proteins, or if their activity is restrained to those Smc5/6-Nse2 molecules directly engaged on DNA, promoting the modification of chromosome-associated targets only. Here we show that DNA stimulates the SUMO ligase activity of Nse2 via a direct and non-specific interaction with a positively-charged patch in the *ARM* region of Smc5. This interaction probably induces a conformational change in the Nse2 molecule that ultimately enhances its SUMO E3 ligase activity, thereby promoting DNA damage repair. Overall, our findings define a new mechanism to activate a SUMO ligase on site, which does not merely rely on recruitment of the E3 to DNA, but on local upregulation of its activity after loading onto chromatin.

RESULTS

DNA binding enhances the SUMO conjugation activity of Nse2

Despite most known SUMO-targets of Nse2 are chromosomal proteins (Zhao & Blobel, 2005; Potts *et al*, 2006; Almedawar *et al*, 2012; McAleenan *et al*, 2012; Albuquerque *et al*, 2013; Andrews *et al*, 2005; Pebernard *et al*, 2008a; Potts & Yu, 2007; Yong-Gonzales *et al*, 2012), it is currently unknown if chromatin loading of Smc5/6 molecules modulates its E3 ligase activity. We therefore tested whether the SUMO conjugation activity of Nse2 could be directly affected by the presence of DNA. In vitro assays using recombinant full-length Smc5 in complex with Nse2 show a substantial increase in SUMO conjugation in the presence of single-stranded DNA (**Fig 1A** and **Fig EV1**). The SUMO E3 ligase activity of Nse2 is strikingly enhanced by the presence of ssDNA, as observed after 30 minutes in multiple turnover reactions. The C-terminal *kleisin* domain of Nse4 (cNse4 - from Ile246 to Asp402) was used as a model substrate in our in vitro reactions, although SUMO conjugation can also be observed internally on lysine residues of Smc5 (**Fig 1A** and **Fig EV1**). These results suggest that DNA binds to the Smc5-Nse2 heterodimer and stimulates the E3 SUMO ligase activity of Nse2. It is important to note that in addition to target selectivity, E3 ligases also optimize catalysis, by placing the functional groups in an optimal orientation for Ub/Ubl transfer between the E2-thioester and the target substrate (Buetow *et al*, 2015; Deshaies & Joazeiro, 2009; Plechanovová *et al*, 2012; Reverter & Lima, 2005; Scott *et al*, 2014; Streich & Lima, 2016).

Most of our in vitro assays utilize single-stranded DNA (ssDNA, 5kb virion ϕx174), which seems to produce a higher increase in SUMO conjugation than a double-stranded DNA plasmid of a similar length (**Fig 1B**), although both types of DNA molecules can produce a substantial increment in SUMO conjugation (**Fig 1B** and **Fig EV1**). Single-stranded DNA has been reported to bind Smc5 and Smc6 molecules with higher affinity than double-stranded DNA through multiple binding sites, including parts of the coiled coil ARM domain (Roy *et al*, 2011, 2015). Additionally, shorter ssDNA molecules, such as random oligonucleotides of 20, 34 and 50 nucleotides, can also enhance SUMO conjugation when used at higher concentrations (μM) than the virion plasmid (nM) in a dose dependent manner (**Fig 1C** and **Fig EV1**). Comparative activity assays using different types of ssDNA molecules at similar nucleotide concentration reveal an equal stimulation of the SUMO conjugation for either oligonucleotides of 50nt or long ssDNA molecules (5kb virion ϕx174 ssDNA) (**Fig 1C**). Small oligonucleotides (20nt) can also enhance SUMO conjugation when used at higher concentrations (**Fig 1C**). These results suggest a non-specific dose-dependent binding of DNA to the Smc5/6 complex resulting in a stimulation of the E3 ligase activity of Nse2.

A minimal Smc5 ARM domain is sufficient for upregulation of DNA-dependent SUMO conjugation

Nse2 has weaker SUMO conjugation activity in the absence of Smc5, with no significant increase in the presence of ssDNA (**Fig 2B**, **2E** and **Appendix Fig S1**). This observation indicates that the Smc5 protein might directly interact with DNA to enhance sumoylation. Smc5 has been reported to bind DNA through multiple binding sites (Roy *et al*, 2011, 2015). Therefore, we mapped the regions in Smc5 responsible for sensing DNA that could enhance SUMO conjugation. We prepared two truncations of Smc5 in complex with Nse2: one lacking the dimerization *HINGE* domain (ΔHinge/Smc5), and another lacking the ATPase *HEAD* domain (ΔHead/Smc5). In both cases the coiled coil domain of Smc5 included the Nse2-binding region (**Fig 2A**). Full-length and Smc5 truncations displayed a comparable and remarkable increase in SUMO conjugation in the presence of DNA (**Fig 2B** and **Appendix Fig S1**). The ΔHinge/Smc5 construct displayed a lower fold increase in sumoylation, most probably due to its already higher activity than wild-type Smc5, even in the absence of DNA (**Fig 2B** and **Appendix Fig S1**). We speculate that the *HINGE* domain may exert an inhibitory role on Nse2-dependent sumoylation. As cNse4 does not interact with either ΔHead/Smc5 or Arm/Smc5 (**Fig Appendix Fig S2**) these assays also indicate that the enhancement of the SUMO E3 ligase activity can occur either on external substrates (such as cNse4), or on internal lysines residues of Smc5 **(Fig 2C**, **2D** and **Appendix Fig S1**). The only common region in all Smc5 constructs corresponds to the *ARM* coiled coil region that docks Nse2 (from Asp302 to Thr366, and from Arg737 to Gln813), indicating that it might contain a minimal DNA-binding region (DNA sensor) that promotes the stimulatory effect on the E3 ligase activity of Nse2.

Therefore, we produced this Smc5 coiled coil *ARM* region (named Arm/Smc5) in complex with Nse2, based on the published crystal structure of Nse2-Smc5 (pdb 3HTK) (Duan *et al*, 2009). Activity assays in the presence or absence of cNse4 also display a striking comparable enhancement in SUMO conjugation upon DNA binding to Arm/Smc5-Nse2*,* similarly to the other Smc5 long truncation constructs (**Fig 2B**, **2E**). These results indicate that the DNA binding patch involved in the enhancement of the E3 ligase might be restricted to this ARM/Smc5 region in contact with Nse2.

A positive-patch region of Smc5 ARM domain interacts with DNA

Similarly to the full-length Smc5-Nse2 complex, different ssDNA molecules can also stimulate SUMO conjugation in the Arm/Smc5-Nse2 construct in a dose-dependent manner (**Fig 3A**). Additionally, single turnover reactions using this minimal

Arm/Smc5-Nse2 construct display a strong enhancement of the E2-thioester SUMO discharge in the presence of a 50nt ssDNA oligonucleotide, indicating the role of the DNA binding promoting the isopeptidic bond formation by the stimulation of the E3 ligase (**Fig 3B)**.

Our next goal was to uncover the DNA binding regions on the surface of the minimal Smc5 ARM domain that can stimulate the activity of Nse2. Interestingly, the crystal structure of the Smc5-Nse2 complex revealed positive-charged patch regions in the Smc5 *coiled coil* surface of Arm/Smc5-Nse2 that could fulfill non-specific interaction to DNA (**Fig 3C**). To check this electrostatic interaction we produced several Arm/Smc5-Nse2 constructs with different combinations of lysine to glutamic acid mutants to countercharge binding to phosphate groups of DNA.

All tested Arm/Smc5-Nse2 KE mutants show a comparable activity in the absence of DNA (**Fig 3D** and **Fig EV2**), indicating in all cases that the mutagenesis has not compromised either the structure or the catalytic properties of the enzyme. However in the presence of DNA, all single point, double, and K337E/K344E/K764E mutants reduce SUMO conjugation at different levels, reaching an almost complete loss of enhancement in the K743E/K745E mutant (**Fig 3D**). Interestingly, the most relevant lysine residues locate in the region next to the RING domain, reducing the effect as they move away from that region. We attribute this decrease in the SUMO E3 ligase activity of Nse2 to an electrostatic perturbation in DNA binding. Also, in contrast to the KE mutants, the SUMO conjugation enhancement of the K743R/K745R double mutant is similar to the wild-type form (**Fig 3D)**, confirming the role of the electrostatic charge of this interface in the DNA binding. Additionally, electrophoretic mobility shift assays (EMSA) using two different Arm/Smc5-Nse2 KE mutants, K337E/K344E/K764E and K743E/K745E, showed a significant reduction of the DNA binding in comparison to the wild-type form, confirming the perturbation of the binding between DNA and the Arm/Smc5-Nse2 complex (**Fig 3E**). These EMSA experiments were conducted at higher DNA:protein ratios in comparison the in vitro activity assays, denoting the unspecific electrostatic binding between *ARM/Smc5* and the DNA molecule.

DNA binding to Smc5-Nse2 triggers a conformational change

The enhancement of the SUMO conjugation upon DNA binding could derive from the structural modification in the Nse2 E3 ligase to stimulate its enzymatic activity. To test this idea we used circular dichroism spectroscopy, which measures the differential absorption of the circularly polarized light. In the far ultraviolet region, this variation arises mainly from changes in the secondary structure elements and is highly sensitive to conformational changes of proteins (Kelly *et al*, 2005).

The circular dichroism analysis of the Arm/Smc5-Nse2 complex displays the spectra of a well-folded α-helical rich protein, with two characteristic ellipticity minimals at 210 and 222 nm, respectively (**Fig 4** and **Appendix Fig S3**). The structural integrity of the complex was confirmed by temperature denaturation after incubation at 100ºC, which resulted in a total loss of the circular dichroism signal (**Fig 4A**). Interestingly, increasing concentrations of DNA (ϕx174) produced a dose-dependent change of the circular dichroism spectra, which might indicate a DNA-induced structural change. Interestingly, the variation of ellipticity displayed by the wild-type spectra was reduced significantly at different levels when four different types of Arm/Smc5-Nse2 KE mutants were used (**Fig 4A** and **Appendix Fig S3**). In all cases the change in the molar ellipticity for the Arm/Smc5-Nse2 KE mutants did not reach the saturation levels displayed by the wild-type form under similar experimental conditions, probably indicating a loss of affinity between DNA molecules and the KE mutants (**Fig 4A**). In summary, all our circular dichroism experiments are indicative of a structural change in the secondary structure elements of Arm/Smc5-Nse2 upon DNA binding.

Taking advantage of the lack of tryptophan residues in the *ARM* region of Smc5, we could follow structural changes in Nse2 by Trp-intrinsic fluorescence, by measuring a red-shift of fluorescence emission upon DNA binding. The two tryptophan residues of Nse2, Trp109 and Trp154, are located in opposite ends of the Nse2 structure and buried in the helical interface with the *ARM* coiled coil structure (**Fig EV3**). Binding of different types of DNA molecules, such as circular ssDNA (5kb) and small ssDNA molecules (20 and 50nt) produce a similar significant red-shift of the Trp fluorescence emission, indicative of a conformational change. In all cases a dose-dependent curve of the fluorescence emission is observed in titration experiments using increasing concentrations of DNA (**Fig 4B**). Interestingly, the equilibrium constants of the saturation curves between the 50nt oligonucleotide and long ssDNA are quite similar (2.7-fold increase). These results are in agreement with our in vitro activity assays for the different types of DNA molecules.

Moreover, four different Arm/Smc5-Nse2 KE mutants can reduce significantly the Trp-fluorescence emission when compared to the wild-type form under similar experimental conditions (**Fig 4C** and **Fig EV3**), probably indicating a loss of affinity between the DNA molecule and the complex. Interestingly, *NaCl*-concentration dependence could be observed in either the Trp-fluorescence emission signal (**Fig 4B**, *inset*), as well as in the SUMO conjugation assays (**Fig EV2**). All our results suggest that the electrostatic interaction between the DNA and the *ARM* domain (DNA sensor), probably through the interaction between the negatively-charged phosphate groups and positively-charged lysine residues, produces a structural change that results in an

enhancement of the SUMO conjugation activity of the Nse2 E3 ligase. Notably, a highly negatively-charged small polymer such as enoxaparin (a low molecular weight heparin) (Lima & de Prat-Gay, 1997) can also stimulate the SUMO E3 ligase activity of Nse2/Smc5 complex in our in vitro conjugation assays (**Fig EV4**), mimicking the non-specific charged-based interaction of the DNA molecules with the DNA sensor of Smc5.

Compromising DNA binding to Smc5 sensitizes yeast cells to DNA damage

To test the relevance of the DNA sensor in vivo, we generated different *SMC5* expression plasmids containing KE mutations. We first focused our attention on K743 and K745 in coiled coil 2, as they seem to more strongly modulate the DNA-dependent activation of Nse2 in vitro (**Fig 3D**). We introduced an *smc5-K743,745E* expressing plasmid, as well as one expressing the *smc5-K743,745R* allele (which does not change the positive charge of the residues), into a conditional *smc5* mutant strain. Yeast growing spot analysis revealed that both mutants support the viability of the conditional allele under non-permissive conditions, indicating that the overall function of the Smc5/6 complex is not substantially affected by the presence of the KE or KR mutations (**Fig EV5**). However, we noticed that while the *K743,745E* mutant rendered cells moderately sensitive to MMS, the *K743,745R* mutant did not. This suggests that the DNA damage sensitivity stems from a change to a negatively-charged residue, rather than mutation of lysines. Despite K764 also seems to be important for DNA-dependent sumoylation in vitro (**Fig 3D**), the sensitivity was not substantially increased in the triple *smc5-K743,745,764E* mutant (*smc5-3KE*) relative to the double *smc5-K743,734E* mutant (**Fig EV5**). On the other hand, *smc5-K337,344E* double mutant cells were not sensitive to DNA damage. Moreover, a quadruple *smc5-K337,K344,K354,K355E* mutant (*smc5-4KE*), containing two other KE mutations close to the *RING* domain of Nse2 (**Fig 3C**), did not substantially affect the DNA damage sensitivity. We next reasoned that, in the context of an integer Smc5/6 complex, positively-charged residues in the Smc5 *ARM* region may act redundantly for interaction with DNA and DNA-dependent activation of Nse2. We therefore generated an allele combining both sets of mutations in the *ARM* domain of Smc5, hereafter referred to as *smc5-7KE* (K337,K344,K354,K355,K743,K745,K764E). Interestingly, growth of the *smc5-7KE* expressing cells was severely impaired in the presence of MMS (**Fig EV5**).

The sensitivity of *KE* mutant cells to MMS resembles that of Nse2 RING mutants (Zhao & Blobel, 2005; Andrews *et al*, 2005), suggesting that mutation of lysines in the DNA-sensor of Smc5 alters the ability of yeast cells to activate the Nse2

SUMO ligase. The *nse2-CH* allele carries the *C200A* and *H202A* RING-disrupting mutations and renders cells sensitive to genotoxic stress (Branzei *et al*, 2006). To directly compare the sensitivity of both type of mutants (*smc5-KE* and *nse2-CH*), we integrated the *KE* alleles into the endogenous *SMC5* locus (see **Fig 5A** for location of mutated lysines). As shown in **Fig 5B**, and in agreement with results from ectopically expressed Smc5 (**Fig EV5**), *smc5-K743,745E* and *smc5-3KE* cells display growth defects in the presence of MMS. The *smc5-7KE* cells exhibit stronger MMS-sensitivity, to levels similar to *nse2-CH* mutant cells. In contrast, *smc5-K743,745R* and *smc5-7KR* mutant cells, which maintain the positive charge of the mutated residues, are not sensitive to MMS (**Fig 5C**). This indicates that the MMS sensitivity in *smc5-KE* cells stems from counter-charge mutations, rather than loss of lysine residues per se. We propose that lysines located in the *ARM* domain of Smc5 synergistically collaborate in the repair of MMS-induced DNA damage.

A DNA sensor in Smc5 participates in sumoylation in vivo

In accordance with the DNA damage sensitivity assays on plates, pull-down of 6his-Flag-tagged SUMO (HF-SUMO) shows that Smc5 sumoylation is diminished in *smc5-3KE* and *smc5-K743,745E* mutants, while it is not affected in *smc5-4KE* cells (**Fig 6A**). The reduced sumoylation in *smc5-K743,745E* cells is not due to mutation of lysine residues, as the *smc5-K743,745R* mutant shows wild-type levels of Smc5-SUMO (**Fig 6A**). Quantification of sumoylated species from SUMO pull downs shows that sumoylation significantly drops to about 60% in *smc5-3KE* mutants (relative to wild-type Smc5; **Fig 6C**). The *smc5-K743,745E* mutation, but not the *smc5-K743,745R* mutant, also affects sumoylation of another Nse2 target, the Sgs1 protein (a homologue of the Bloom's and Werner's syndrome genes and a member of the STR complex) (Bermúdez-López *et al*, 2016). This finding indicates that the DNA sensor is also required to increase sumoylation of protein targets outside the Smc5/6 complex (**Appendix Fig S4**).

On the other hand, the *smc5-7KE* allele had a stronger effect on Smc5 sumoylation, which further dropped to about one third of wild-type levels (**Fig 6B and 6C**). This effect does not simply depend on loss of lysine residues, as the smc5-7KR mutant protein displayed higher levels of sumoylation than smc5-7KE (**Fig 6B**, right panel). However, we also noted that sumoylation of the smc5-7KR protein was lower than its wild-type counterpart. We speculate that the partial reduction in the sumoylation levels of the smc5-7KR protein might be due to loss of potential SUMO acceptor sites. To directly compare sumoylation levels in *KE* and *nse2* mutant cells, we used an *nse2⊿C* mutant strain, carrying a deletion in the C-terminal RING domain. As

shown in **Appendix Fig S4**, SUMO pull down analysis indicates a low and similar level of sumoylation for both *smc5-7KE* and *nse2⊿C* cells, relative to wild-type cells, and a more modest reduction in the *smc5-3KE* strain.

As *KE* mutations lay close to the Nse2 binding domain in Smc5, it is possible that the diminished sumoylation in *smc5-KE* mutants is due to reduced Smc5-NSe2 association. However, co-immunoprecipitation experiments indicate that the smc5-3KE and smc5-7KE proteins bind efficiently to the Nse2 SUMO ligase (**Fig 6D**). On the other hand, while the smc5-3KE mutant protein shows wild-type levels of association with Smc6, smc5-7KE competes less efficiently for binding to Smc6 (**Fig 6E**). This observation suggests that the *smc5-7KE* allele might compromise the stability of the Smc5/6 complex.

Finally, to analyze if the sumoylation defects of *KE* mutants stem from deficient recruitment to chromatin, we tested chromosomal association of Smc5-6HA by immunofluorescence on chromosome spreads. As shown in **Fig 6F**, there are no significant changes in chromatin binding between wild-type and mutant Smc5-3KE proteins. These data suggest that DNA sensing by the positively-charged patch in the coiled coil of Smc5 occurs after loading of the Smc5/6 complex onto chromatin. In contrast, the extended *smc5-7KE* DNA sensor mutant shows significantly reduced chromatin association, relative to wild-type Smc5 (**Fig 6F)**. We speculate that this decrease might be due to the combined action of, among others, defective interaction with DNA in the ARM domain, loss of putative acceptor lysines in Smc5 and compromised stability of the Smc5/6 complex.

Overall, we conclude that K743 and K745 represent a minimal positively charged patch in the Smc5 molecule, which acts as a DNA sensor in yeast, able to interact with DNA and to promote the activity of the Nse2 SUMO ligase thus ensuing repair of MMS-induced DNA damage.

DISCUSSION

Many aspects of chromosome replication, repair and segregation require post-translational modification by SUMO to maintain the integrity of the genome (Bergink & Jentsch, 2009). A plethora of SUMO-targeted chromosome-associated proteins, many of them involved in nucleic acid metabolism, has been identified in recent proteomic screens (Cubeñas-Potts *et al*, 2015; Lamoliatte *et al*, 2014; Tatham *et al*, 2011). Preferential sumoylation of chromosome-associated proteins raises the mechanistic question of what promotes 'on-site sumoylation' (Ulrich, 2014; Sarangi & Zhao, 2015). It has been proposed that specific sumoylation of chromosome-bound targets requires either the recruitment of the SUMO E3 ligase to chromatin or DNA-dependent structural changes in the substrate to make it amenable to modification (Ulrich, 2014; Sarangi & Zhao, 2015). Here, we show a novel regulatory mechanism that can account for 'on-site' sumoylation, based on the stimulation of the Nse2 SUMO ligase in the Smc5/6 complex by DNA. Our proposed mechanism differs from a few other cases in which DNA binding affects SUMO conjugation, even in the absence of a E3 ligase, i. e. enhanced affinity of PARP-1 for E2-SUMO thioester upon DNA binding (Zilio *et al*, 2013); stimulation of SUMO conjugation of PCNA when loaded to DNA (Parker *et al*, 2008). In our model the stimulation requires non-specific binding of DNA to a positively-charged patch in the coiled coil of Smc5 (DNA-sensor), which subsequently mediates a conformational change in the SUMO ligase. This mechanism is ideal to promote sumoylation of Smc5/6-dependent targets on site and to elude the modification of targets not directly engaged on chromatin.

Although it is formally unproven that modification of Smc5/6-Nse2 targets occurs on chromatin, circumstantial evidence suggests that it is highly probable. For example, Smc5/6 binds to damaged loci such as double-strand breaks (Lindroos *et al*, 2006; De Piccoli *et al*, 2006) and stalled replication forks (Bustard *et al*, 2012), but also to ribosomal DNAs repeats, telomeres and centromeres (Pebernard *et al*, 2008b; Lindroos *et al*, 2006; Jeppsson *et al*, 2014; Torres-Rosell *et al*, 2005); not surprisingly, most Smc5/6-Nse2 targets are enriched at these sites. It is worth noting that DSBs, telomeres, and stalled replication forks are characterized by the accumulation of ssDNA. Smc5-Smc6 heterodimeric molecules have a higher affinity for ssDNA than for dsDNA (Roy *et al*, 2015), suggesting that their localization to these sites, and the consequent upregulation of sumoylation, may be partly driven by the intrinsic affinity of the SMC core for ssDNA. Although both single- and double-stranded DNA molecules are capable of potentiating sumoylation, our observations indicate that ssDNA has a somewhat stronger effect than dsDNA. Consequently, we speculate that the enhancement of the E3 ligase activity by DNA might be partially responsible for the

upregulation of protein sumoylation upon DNA damage, as the latter normally induces the accumulation of ssDNA. Of note, Smc5-Smc6 heterodimers have a higher affinity for ssDNA than the Rad51 recombinase (Roy *et al*, 2015), suggesting that they might even outcompete the later for binding to single-stranded DNA fibers. It is also worth noting that the Nse1-Nse3 subcomplex displays higher affinity for dsDNA than for ssDNA in vitro (Zabrady *et al*, 2016b). Hence, further experiments will be required to assess whether ssDNA plays a preferential role in sumoylation of Smc5/6-Nse2 targets.

One of the most striking effects observed in this study is the absence of DNA-dependent effects on Nse2 ligase activity (**Fig 2E** and **Appendix Fig S1**). This finding indicates that docking to the Smc5/6 complex has a positive influence on Nse2-dependent sumoylation. We currently cannot discard that other regions in the Smc5/6 complex, different from the DNA-sensor described here, participate and/or modulate the effect of DNA on the E3 ligase activity. Still, we have shown that the *ARM* region in the Smc5 molecule is sufficient to confer the DNA-dependency in vitro. Interestingly, the analysis of Smc5 truncations indicates that other domains in the molecule also modulate the E3 ligase, although in a completely different manner: removal of the *HINGE* domain in Smc5 leads to a higher sumoylation level, suggesting that the hinge physically obstructs sumoylation (**Fig 2**). Thus, one attractive possibility is that the association of DNA with the hinge (Alt *et al*, 2017) primes the subsequent DNA-dependent activation of the E3 ligase. This suggests a two-step model for DNA association with Smc5, first through the *HINGE* domain and, after removal of the hindrance, with the DNA sensor in the *ARM* domain.

We have analyzed two different substrates to study the DNA-dependent activation of the Nse2 SUMO ligase in vitro: (i) internal lysines of the Smc5 protein, which have already been reported to be intrinsically sumoylated by Nse2 (Zhao & Blobel, 2005); and (ii) the C-terminal kleisin domain of Nse4 (cNse4), which binds to the ATPase *HEAD* domain of Smc5 and does not interact with either the *ARM* or the *HINGE* domains (**Appendix Fig S2**). Nse4 sumoylation proceeds in trans (in opposition to E3 auto-sumoylation), and can thus be considered an external substrate (Pichler *et al*, 2017); this is particularly evident under conditions where Nse4 does not interact with either Smc5 or Nse2 (for example, in ΔHead/Smc5 or Arm/Smc5 truncations; **Fig 2**). Sumoylation of Smc5 and cNse4 is equally enhanced by binding to different types of DNA (ssDNA and dsDNA) in a dose-dependent manner. The proximity of the DNA-sensor in Smc5 to the *RING* domain of Nse2, should facilitate the enhancement of the SUMO E3 ligase activity. In accordance, Trp-intrinsic fluorescence and circular dichroism indicate structural remodelling of the Smc5-Nse2 complex upon

DNA binding. Interestingly, our DNA titration by circular dichroism is analogous to the CpG DNA binding to the Toll-like Receptor 9 ectodomain (Latz *et al*, 2007), in both cases resulting in a similar DNA dose-dependent modification of the CD spectra.

Crystallographic studies have proven the role of the RING domain of E3 ligases in the recruitment of the charged E2-conjugating enzyme, whereby a simultaneous interaction with SUMO (or ubiquitin) and the E2 enzyme would enhance the catalytic reaction. Thus, it is feasible to conceive a structural reorientation of the RING domain in Nse2 that would facilitate either the interaction with the E2-conjugating enzyme or the transfer to the substrate, as proposed here. Structural data on the rearrangement of the Smc5-Nse2 structure in the presence of DNA will be extremely useful to prove it.

The phenotypes displayed by the KE point mutants in the Smc5 DNA-sensor patch are reminiscent of mutants in the *RING* domain of Nse2, affecting cell growth in the presence of genotoxic agents. We propose that the K743 and K745 residues constitute a minimal DNA sensor involved in activation of the SUMO ligase. Although other lysines in the Smc5-ARM domain might have a synergistic effect on DNA binding in vivo, the *smc5-7KE* mutant might disturb natural lysine acceptor sites. Additionally, it is possible that the extended positively charged patch participates in other functions not directly related to sumoylation, including Smc5/6 complex stability; in accordance with this notion, the smc5-7KE mutant protein shows reduced chromatin binding and reduced association with Smc6 (**Fig 6E** and **F**).

We propose that both *KE* and *RING* mutants compromise the enzymatic activity of the Nse2 SUMO E3 ligase, either by preventing the interaction with the E2 enzyme (in the case *RING* domain mutants) or by perturbing the association of DNA with the Smc5 DNA-sensor (in DNA-sensor patch mutants). It is worth noting that the *KE* DNA-sensor mutants only disrupt regulation of the E3 by DNA, and do not affect the basal activity of the E3 ligase (**Fig 3D**). We propose that the moderate DNA damage sensitivity of *smc5-K743,745E* and *smc5-3KE* cells corresponds to an Smc5/6 complex that has impaired DNA-dependent enhancement of sumoylation but carries a functional E3 ligase; the higher MMS sensitivity of *nse2* mutants would correlate to a situation of severely impaired sumoylation. We predict that most chromosome-bound Nse2 targets (Potts *et al*, 2006; Bermúdez-López *et al*, 2015; Almedawar *et al*, 2012; McAleenan *et al*, 2012; Bermúdez-López *et al*, 2016; Bonner *et al*, 2016), including cohesin, the Sgs1-Top3-Rmi1 complex and the Smc5/6 complex itself will be regulated by this mechanism. Thus, we propose that a reduced sub-optimal level of sumoylation in Nse2 targets accounts for the MMS sensitivity of *smc5-KE* mutant cells.

In addition to the DNA-dependent enhancement of the SUMO E3 ligase activity, we cannot underestimate the contribution played by the DNA molecule in bringing

Smc5/6 molecules in close proximity to its substrates. In fact, we have observed a non-specific binding of the C-terminal kleisin domain of Nse4 (cNse4) to DNA in EMSA experiments (**Appendix Fig S2**), although this interaction is only observed at protein:DNA ratios much higher than those able to induce the structural rearrangement and activation of the ligase. Nevertheless, a scaffolding function of DNA cannot account for all the effects observed in vitro as: (i) short DNA molecules should substantially reduce the probability of enzyme-substrate co-binding to the same DNA molecule, a prediction that is not observed when comparing 5kb- and 50nt-long ssDNAs (**Fig 1C**); (ii) both sumoylation and conformational changes can be promoted by enoxaparin, a small negatively-charged molecule, pointing to electrostatic interactions as activators of sumoylation (**Fig EV4**); and (iii) our in vivo data indicates that Smc5/6 complexes loaded on chromatin are less active when mutated in their DNA sensor (*smc5-3KE* mutant in **Fig 6A** and **F**). Moreover, ATPase mutant Smc5/6 complexes show diminished SUMO E3 activity. The dependence on the ATPase activity is probably two-fold: binding to ATP promotes a conformational change in the Smc5-Nse2 molecule that stimulates its SUMO-ligase activity (Bermúdez-López *et al*, 2015); additionally, binding to ATP regulates the association of the Smc5/6 holocomplex with DNA (Kanno *et al*, 2015) what, according to the results presented here, further enhances its SUMO ligase activity. Therefore, we speculate that the Smc5/6 complex can be first activated by ATP-dependent remodeling of the molecule and loading onto DNA; this would facilitate contacts between DNA and the DNA-sensor patch in Smc5, which would subsequently activate the SUMO E3 ligase activity of Nse2 (**Fig 7**). This mechanism should help to confine the activity of a critical E3 ligase towards substrates pre-loaded on chromatin and bound to the same stretch of DNA. It is worth noting that the ATPase activity in bacterial SMC complexes may regulate the dynamic association with DNA by altering the conformation of the coiled coil domains (Bürmann *et al*, 2017). As the Nse2 SUMO ligase docks to the coiled coil domain of Smc5, it is possible that the ATPase in the Smc5/6 complex might not only alter the juxtaposition of the coiled coils (Bürmann *et al*, 2017; Alt *et al*, 2017), but also promote the concomitant activation of Nse2 after entrapment of DNA inside the Smc5/6 ring.

In summary, we have revealed a novel mechanism regulating a SUMO E3 ligase activity both by localization, occurring only upon association with DNA, and by the structural rearrangement of the E3 ligase. Given the prominent role played by ubiquitin and ubiquitin-like ligases in genome integrity, it will be very interesting to know if other E3s operating on chromosome-associated proteins employ analogous mechanisms.

Author contributions: NV, JL and DR conducted all SUMO conjugation in vitro experiments. NV conducted the circular dichroism and fluorescence analysis. EI, NC and JTR conducted the in vivo yeast experiments. DR and JTR analyzed the results and wrote the paper. DR and JTR conceived the idea for the project.

Conflict of interest: The authors declare that they have no conflicts of interest with the contents of this article.

Acknowledgements: We thank Xiaolan Zhao for kindly providing the *nse2-CH* allele. Members of our labs for discussions; Chris Lima and Luis Aragon for critical reading of the manuscript. This work was supported by grants from the “Ministerio de Economia y Competitividad” BFU2015-66417-P (MINECO/FEDER) to DR and grants BFU2015-71308-P and BFU2013-50245-EXP to JTR. NV acknowledges the support from the Science Without Borders (CNPq, Brazil).

REFERENCES

Albuquerque CP, Wang G, Lee NS, Kolodner RD, Putnam CD & Zhou H (2013) Distinct SUMO ligases cooperate with Esc2 and Slx5 to suppress duplication-mediated genome rearrangements. *PLoS Genet.* **9:** e1003670

Almedawar S, Colomina N, Bermúdez-López M, Pociño-Merino I & Torres-Rosell J (2012) A SUMO-dependent step during establishment of sister chromatid cohesion. *Curr. Biol.* **22:** 1576–81

Alt A, Dang HQ, Wells OS, Polo LM, Smith MA, McGregor GA, Welte T, Lehmann AR, Pearl LH, Murray JM & Oliver AW (2017) Specialized interfaces of Smc5/6 control hinge stability and DNA association. *Nat. Commun.* **8:** 14011

Alva V, Nam S-Z, Söding J & Lupas AN (2016) The MPI bioinformatics Toolkit as an integrative platform for advanced protein sequence and structure analysis. *Nucleic Acids Res.* **44:** W410–W415

Ampatzidou E, Irmisch A, O'Connell MJ & Murray JM (2006) Smc5/6 is required for repair at collapsed replication forks. *Mol. Cell. Biol.* **26:** 9387–401

Andrews EA, Palecek J, Sergeant J, Taylor E, Lehmann AR & Watts FZ (2005) Nse2, a component of the Smc5-6 complex, is a SUMO ligase required for the response to DNA damage. *Mol. Cell. Biol.* **25:** 185–96

Behlke-Steinert S, Touat-Todeschini L, Skoufias DA & Margolis RL (2009) SMC5 and MMS21 are required for chromosome cohesion and mitotic progression. *Cell Cycle* **8:** 2211–2218

Bergink S & Jentsch S (2009) Principles of ubiquitin and SUMO modifications in DNA repair. *Nature* **458:** 461–467

Bermúdez-López M, Pociño-Merino I, Sánchez H, Bueno A, Guasch C, Almedawar S, Bru-Virgili S, Garí E, Wyman C, Reverter D, Colomina N & Torres-Rosell J (2015) ATPase-Dependent Control of the Mms21 SUMO Ligase during DNA Repair. *PLoS Biol.* **13:**

Bermúdez-López M, Villoria MT, Esteras M, Jarmuz A, Torres-Rosell J, Clemente-Blanco A & Aragon L (2016) Sgs1's roles in DNA end resection, HJ dissolution, and crossover suppression require a two-step SUMO regulation dependent on Smc5/6. *Genes Dev.* **30:** 1339–1356

Bernier-Villamor V, Sampson DA, Matunis MJ & Lima CD (2002) Structural basis for E2-mediated SUMO conjugation revealed by a complex between ubiquitin-conjugating enzyme Ubc9 and RanGAP1. *Cell* **108:** 345–56

Bonner JN, Choi K, Xue X, Torres NP, Szakal B, Wei L, Wan B, Arter M, Matos J, Sung P, Brown GW, Branzei D & Zhao X (2016) Smc5/6 Mediated Sumoylation of the

Sgs1-Top3-Rmi1 Complex Promotes Removal of Recombination Intermediates. *Cell Rep.* **16:** 368–378

Branzei D, Sollier J, Liberi G, Zhao X, Maeda D, Seki M, Enomoto T, Ohta K & Foiani M (2006) Ubc9- and Mms21-Mediated Sumoylation Counteracts Recombinogenic Events at Damaged Replication Forks. *Cell* **127:** 509–522

Buetow L, Gabrielsen M, Anthony NG, Dou H, Patel A, Aitkenhead H, Sibbet GJ, Smith BO & Huang DT (2015) Activation of a primed RING E3-E2-ubiquitin complex by non-covalent ubiquitin. *Mol. Cell* **58:** 297–310

Bürmann F, Basfeld A, Vazquez Nunez R, Diebold-Durand ML, Wilhelm L & Gruber S (2017) Tuned SMC Arms Drive Chromosomal Loading of Prokaryotic Condensin. *Mol. Cell*

Bustard DE, Menolfi D, Jeppsson K, Ball LG, Dewey SC, Shirahige K, Sjögren C, Branzei D & Cobb JA (2012) During replication stress, non-SMC element 5 (NSE5) is required for Smc5/6 protein complex functionality at stalled forks. *J. Biol. Chem.* **287:** 11374–83

Chavez A, George V, Agrawal V & Johnson FB (2010) Sumoylation and the structural maintenance of chromosomes (Smc) 5/6 complex slow senescence through recombination intermediate resolution. *J. Biol. Chem.* **285:** 11922–30

Chung I & Zhao X (2015) DNA break-induced sumoylation is enabled by collaboration between a SUMO ligase and the ssDNA-binding complex RPA. *Genes Dev.* **29:** 1593–8

Colomina N, Guasch C & Torres-Rosell J (2017) Analysis of SUMOylation in the RENT Complex by Fusion to a SUMO-Specific Protease Domain. In *Methods in molecular biology (Clifton, N.J.)* pp 97–117.

Cremona CA, Sarangi P, Yang Y, Hang LE, Rahman S & Zhao X (2012) Extensive DNA Damage-Induced Sumoylation Contributes to Replication and Repair and Acts in Addition to the Mec1 Checkpoint. *Mol. Cell* **45:** 422–432

Cubeñas-Potts C, Srikumar T, Lee C, Osula O, Subramonian D, Zhang X-D, Cotter RJ, Raught B & Matunis MJ (2015) Identification of SUMO-2/3-modified proteins associated with mitotic chromosomes. *Proteomics* **15:** 763–772

Deshaies RJ & Joazeiro CA (2009) RING domain E3 ubiquitin ligases. *Annu Rev Biochem* **78:** 399–434

Duan X, Sarangi P, Liu X, Rangi GK, Zhao X & Ye H (2009) Structural and Functional Insights into the Roles of the Mms21 Subunit of the Smc5/6 Complex. *Mol. Cell* **35:** 657–668

Foguel D & Silva JL (1994) Cold denaturation of a repressor-operator complex: the role of entropy in protein-DNA recognition. *Proc. Natl. Acad. Sci. U. S. A.* **91:** 8244–7

Jeppsson K, Kanno T, Shirahige K & Sjögren C (2014) The maintenance of chromosome structure: positioning and functioning of SMC complexes. *Nat. Rev. Mol. Cell Biol.* **15:** 601–614

Johnson ES & Gupta AA (2001) An E3-like factor that promotes SUMO conjugation to the yeast septins. *Cell* **106:** 735–44

Kanno T, Berta DG & Sjögren C (2015) The Smc5/6 Complex Is an ATP-Dependent Intermolecular DNA Linker. *Cell Rep.* **12:** 1471–82

Kelly SM, Jess TJ & Price NC (2005) How to study proteins by circular dichroism. *Biochim. Biophys. Acta - Proteins Proteomics* **1751:** 119–139

Lamoliatte F, Caron D, Durette C, Mahrouche L, Maroui MA, Caron-Lizotte O, Bonneil E, Chelbi-Alix MK & Thibault P (2014) Large-scale analysis of lysine SUMOylation by SUMO remnant immunoaffinity profiling. *Nat. Commun.* **5:** 5409

Latz E, Verma A, Visintin A, Gong M, Sirois CM, Klein DCG, Monks BG, McKnight CJ, Lamphier MS, Duprex WP, Espevik T & Golenbock DT (2007) Ligand-induced conformational changes allosterically activate Toll-like receptor 9. *Nat. Immunol.* **8:** 772–779

Lima LM & de Prat-Gay G (1997) Conformational changes and stabilization induced by ligand binding in the DNA-binding domain of the E2 protein from human papillomavirus . *J Biol Chem* **272:** 19295–19303

Lindroos HB, Ström L, Itoh T, Katou Y, Shirahige K & Sjögren C (2006) Chromosomal association of the Smc5/6 complex reveals that it functions in differently regulated pathways. *Mol. Cell* **22:** 755–67

McAleenan A, Cordon-Preciado V, Clemente-Blanco A, Liu I-C, Sen N, Leonard J, Jarmuz A & Aragón L (2012) SUMOylation of the α-kleisin subunit of cohesin is required for DNA damage-induced cohesion. *Curr. Biol.* **22:** 1564–75

Motulsky HJ & Christopoulos A (2003) Fitting models to biological data using linear and nonlinear regression. *GraphPad Software, Inc., San Diego, CA***:** 351 pp.

Parker JL, Bucceri A, Davies AA, Heidrich K, Windecker H & Ulrich HD (2008) SUMO modification of PCNA is controlled by DNA. *EMBO J.* **27:** 2422–31

Pebernard S, Perry JJP, Tainer JA & Boddy MN (2008a) Nse1 RING-like domain supports functions of the Smc5-Smc6 holocomplex in genome stability. *Mol. Biol. Cell* **19:** 4099–109

Pebernard S, Schaffer L, Campbell D, Head SR & Boddy MN (2008b) Localization of Smc5/6 to centromeres and telomeres requires heterochromatin and SUMO, respectively. *EMBO J.* **27:** 3011–23

De Piccoli G, Cortes-Ledesma F, Ira G, Torres-Rosell J, Uhle S, Farmer S, Hwang J-Y, Machin F, Ceschia A, McAleenan A, Cordon-Preciado V, Clemente-Blanco A,

Vilella-Mitjana F, Ullal P, Jarmuz A, Leitao B, Bressan D, Dotiwala F, Papusha A, Zhao X, et al (2006) Smc5-Smc6 mediate DNA double-strand-break repair by promoting sister-chromatid recombination. *Nat. Cell Biol.* **8:** 1032–4

Pichler A, Fatouros C, Lee H & Eisenhardt N (2017) SUMO conjugation – a mechanistic view. *Biomol. Concepts* **8:** 13–36

Plechanovová A, Jaffray EG, Tatham MH, Naismith JH & Hay RT (2012) Structure of a RING E3 ligase and ubiquitin-loaded E2 primed for catalysis. *Nature* **489:** 115–120

Potts PR, Porteus MH & Yu H (2006) Human SMC5/6 complex promotes sister chromatid homologous recombination by recruiting the SMC1/3 cohesin complex to double-strand breaks. *EMBO J.* **25:** 3377–3388

Potts PR & Yu H (2007) The SMC5/6 complex maintains telomere length in ALT cancer cells through SUMOylation of telomere-binding proteins. *Nat. Struct. Mol. Biol.* **14:** 581–90

Psakhye I & Jentsch S (2012) Protein group modification and synergy in the SUMO pathway as exemplified in DNA repair. *Cell* **151:** 807–20

Räschle M, Smeenk G, Hansen RK, Temu T, Oka Y, Hein MY, Nagaraj N, Long DT, Walter JC, Hofmann K, Storchova Z, Cox J, Bekker-Jensen S, Mailand N & Mann M (2015) DNA repair. Proteomics reveals dynamic assembly of repair complexes during bypass of DNA cross-links. *Science* **348:** 1253671

Reverter D & Lima CD (2005) Insights into E3 ligase activity revealed by a SUMO-RanGAP1-Ubc9-Nup358 complex. *Nature* **435:** 687–92

Roy M-A & D'Amours D (2011) DNA-binding properties of Smc6, a core component of the Smc5–6 DNA repair complex. *Biochem. Biophys. Res. Commun.* **416:** 80–85

Roy M-A, Dhanaraman T & D'Amours D (2015) The Smc5-Smc6 heterodimer associates with DNA through several independent binding domains. *Sci. Rep.* **5:** 9797

Roy MA, Siddiqui N & D'Amours D (2011) Dynamic and selective DNA-binding activity of Smc5, a core component of the Smc5-Smc6 complex. *Cell Cycle* **10:** 690–700

Sarangi P & Zhao X (2015) SUMO-mediated regulation of DNA damage repair and responses. *Trends Biochem. Sci.* **40:** 233–242

Schneider CA, Rasband WS & Eliceiri KW (2012) NIH Image to ImageJ: 25 years of image analysis. *Nat. Methods* **9:** 671–5

Scott DC, Sviderskiy VO, Monda JK, Lydeard JR, Cho SE, Harper JW & Schulman BA (2014) Structure of a RING E3 trapped in action reveals ligation mechanism for the ubiquitin-like protein NEDD8. *Cell* **157:** 1671–84

Silva JL, Miles EW & Weber G (1986) Pressure dissociation and conformational drift of

the beta dimer of tryptophan synthase. *Biochemistry* **25:** 5780–5786

Streich FC & Lima CD (2016) Capturing a substrate in an activated RING E3/E2-SUMO complex. *Nature* **536:** 304–8

Tapia-Alveal C & O'Connell MJ (2011) Nse1-dependent recruitment of Smc5/6 to lesion-containing loci contributes to the repair defects of mutant complexes. *Mol. Biol. Cell* **22:** 4669–82

Tatham MH, Matic I, Mann M & Hay RT (2011) Comparative Proteomic Analysis Identifies a Role for SUMO in Protein Quality Control. *Sci. Signal.* **4:** rs4-rs4

Torres-Rosell J, Machín F, Farmer S, Jarmuz A, Eydmann T, Dalgaard JZ & Aragón L (2005) SMC5 and SMC6 genes are required for the segregation of repetitive chromosome regions. *Nat. Cell Biol.* **7:** 412–419

Uhlmann F (2016) SMC complexes: from DNA to chromosomes. *Nat. Rev. Mol. Cell Biol.* **17:** 399–412

Ulrich HD (2014) Two-way communications between ubiquitin-like modifiers and DNA. *Nat. Struct. Mol. Biol.* **21:** 317–324

Yong-Gonzales V, Hang LE, Castellucci F, Branzei D & Zhao X (2012) The Smc5-Smc6 complex regulates recombination at centromeric regions and affects kinetochore protein sumoylation during normal growth. *PLoS One* **7:** e51540

Yunus A a & Lima CD (2006) Lysine activation and functional analysis of E2-mediated conjugation in the SUMO pathway. *Nat. Struct. Mol. Biol.* **13:** 491–499

Yunus AA & Lima CD (2005) Purification and activity assays for Ubc9, the ubiquitin-conjugating enzyme for the small ubiquitin-like modifier SUMO. *Methods Enzymol.* **398:** 74–87

Zabrady K, Adamus M, Vondrova L, Liao C, Skoupilova H, Novakova M, Jurcisinova L, Alt A, Oliver AW, Lehmann AR & Palecek JJ (2016a) Chromatin association of the SMC5/6 complex is dependent on binding of its NSE3 subunit to DNA. *Nucleic Acids Res.* **44:** 1064–79

Zabrady K, Adamus M, Vondrova L, Liao C, Skoupilova H, Novakova M, Jurcisinova L, Alt A, Oliver AW, Lehmann AR & Palecek JJ (2016b) Chromatin association of the SMC5/6 complex is dependent on binding of its NSE3 subunit to DNA. *Nucleic Acids Res.* **44:** 1064–1079

Zhao X & Blobel G (2005) A SUMO ligase is part of a nuclear multiprotein complex that affects DNA repair and chromosomal organization. *Proc. Natl. Acad. Sci. U. S. A.* **102:** 4777–82

Zilio N, Williamson CT, Eustermann S, Shah R, West SC, Neuhaus D & Ulrich HD (2013) DNA-dependent SUMO modification of PARP-1. *DNA Repair (Amst).* **12:** 761–773

Figure Legends

Figure 1. Stimulation of the SUMO E3 ligase activity of the Smc5-Nse2 complex upon binding to DNA. (A) Time-course SUMO conjugation reaction in the presence or absence of ssDNA (virion ϕx174) using recombinant full-length Smc5-Nse2 complex. The substrate utilized was the C-terminal *kleisin* domain of Nse4 (*cNse4*). Reaction was run at 30°C and stopped at indicated minutes by adding SDS-loading buffer. Labels indicate the bands in the SDS-PAGE of the proteins in the reaction mixture (*N-S2, cNse4-SUMO2; N-2S2, cNse4-2SUMO2 and N-3S2, cNse4-3SUMO2*). **(B) Left**, SYPRO-stained and western-blot (anti-SUMO2) of the SUMO conjugation reaction by Smc5-Nse2 complex in the presence of ssDNA (virion ϕx174) and dsDNA (pET-DUET-1) at either 1 or 10 nM. Reactions were run at 30°C and stopped at 60 minutes by adding SDS-loading buffer. **Right**, bar diagram comparison of the relative SUMO conjugated cNse4 substrate in the presence of either ssDNA (virion ϕx174) or dsDNA (pET-DUET-1) at indicated concentrations. Straight line shows the basal cNse4-SUMO conjugation in the absence of DNA. Data values are mean ± s.e.m. and n=3 technical replicates. **(C) Left**, western-blot of the SUMO conjugation reaction in the presence of 50nt oligonucleotide and the 5 kb virion ϕx174 at the indicated concentrations. Reactions were run at 30°C and stopped after 60 minutes by adding SDS-loading buffer. **Right**, bar diagram comparison of the relative SUMO conjugated cNse4 substrate in the presence of 25, 34 or 50 bases oligonucleotides at indicated concentrations. Straight line shows the basal cNse4-SUMO conjugation in the absence of DNA. Data values are mean ± s.e.m. and n=3 technical replicates. Bar diagrams calculation was generated using ImageJ software (Schneider *et al*, 2012).

Figure 2. Enhancement of the SUMO E3 ligase activity upon DNA binding by Smc5-Nse2 truncation complexes. (A) Schematic representation of the domain composition of the heterodimeric full-length Smc5-Nse2 complex. **(B)** Bar diagram representation of the relative SUMO conjugation activity of Nse2, full-length Smc5-Nse2, ΔHinge/Smc5-Nse2, ΔHead/Smc5-Nse2 and Arm/Smc5-Nse2 truncation constructs (schematic representation above). Orange bar indicate the presence of ssDNA (virion ϕx174) and red bars absence of ssDNA. Reactions rates were performed at least in three different independent experiments (see *Figure S2A*). Data values are mean ± s.e.m; and n=3 technical replicates. Significance was measured by a two-tailed unpaired t-test relative to wild-type. ***P*<0.01. **(C)** SYPRO-stained (**left**) and western-blot (**right**) time course SUMO conjugation reaction using and

ΔHead/Smc5-Nse2 truncation construct in the presence of ssDNA. T7-tagged Smc5 and E1 were immunodetected by an anti-T7 antibody. Reactions were run at 30 °C and stopped at indicated times by adding SDS-loading buffer. **(D)** SYPRO-stained (**left**) and western-blot (**right**) time course SUMO conjugation reaction using and ΔHinge/Smc5-Nse2 truncation construct in the presence of ssDNA. T7-tagged Smc5 and E1 were immunodetected by an anti-T7 antibody. Reactions were run at 30 °C and stopped at indicated times by adding SDS-loading buffer. **(E)** Western-blot of the time-course SUMO conjugation reaction in the presence of ssDNA (virion ϕx174) using either Nse2 (left) or Arm/Smc5-Nse2 complex (right). The reactions were run in the presence or absence of *cNse4* external substrate. Reaction was run at 30°C and stopped at indicated minutes by adding SDS-loading buffer. (*N-S2, cNse4-SUMO2; N-2S2, cNse4-2SUMO2; N-3S2, cNse4-3SUMO2 and pS2, poly-SUMO2*).

Figure 3. A positive-patch region on the surface of Smc5 ARM domain interacts with DNA. (A) Western-blot of the SUMO conjugation reaction in the presence of different oligonucleotides. Reactions were run at 30°C and stopped after 60 minutes by adding SDS-loading buffer. 25b (μM), 34b (μM) and 50b (μM), stands for a 25, 34 and 50 bases oligonucleotides, respectively, and the indicated concentration is in μM units. 5kb (nM), stands for the virion ϕx174 and the indicated concentration is in nM units. (*N-S1, cNse4-SUMO1; N-2S1, cNse4-2SUMO1; and pS1, poly-SUMO1*). **(B) Left,** Ubc9-thioester formation in the presence of E1, E2 enzymes, Alexa488-SUMO1 and ATP. **Right**, single turnover reaction of the SUMO conjugation reaction in the presence or absence of ssDNA (50nt) using Arm/Smc5-Nse2 as E3. Samples were run in the presence (**below**) or absence of β-mercaptoethanol (**above**). **(C)** Ribbon representation of the complex between the *ARM* domain of Smc5 (yellow and orange) and Nse2 (pink) (PDB *3HTK*) (Duan *et al*, 2009). Lysine residues forming the positive-charged patch in the surface of the coiled-coil Smc5 *ARM* are labeled and shown in stick representation (blue). Zinc atom in the Nse2 *RING* domain is depicted as a yellow sphere. **(D)** Bar diagram representation of the SUMO conjugation rates of activity assays of Arm/Smc5-Nse2 KE mutants in the presence (orange bars) or absence (red bars) of ssDNA (virion ϕx174), relative to wild-type (set to 1). Reactions rates were performed at least in three different independent experiments. Data values are mean ± s.e.m and n=3 technical replicates. Significance was measured by a two-tailed unpaired t-test relative to wild-type. **P*<0.05, ***P*<0.01, ****P*<0.001. **(E)** DNA binding properties of wild-type, K337E/K344E/K764E and K743E/K745E Arm/Smc5-Nse2 mutants, were determined by electrophoretic mobility shift assays (EMSA) saturation experiments. Protein complexes were incubated for 30 minutes at 30°C before loading

the agarose gel electrophoresis. Numbers above gel indicate the molar ratio ($x10^3$) of protein over ssDNA (virion ϕx174) in each lane.

Figure 4. Binding of DNA induces distinct conformational changes in Arm/Smc5-Nse2 wild-type and mutants. (A) Left, circular dichroism (CD) analysis of purified wild-type Arm/Smc5-Nse2. Black line, wild-type Arm/Smc5-Nse2 without bound ligand (no 5kb ssDNA); dashed black line, denatured protein; blue line, ligand/Smc5-Nse2; numbers in graphs (dotted black lines), molar ratio of ligand/Smc5-Nse2. **Right**, conformational changes induced by 5kb circular ssDNA quantified by ligand titration until signal change in mean residue ellipticity (MRE) at 222 nm achieved saturation. Blue squares Arm/Smc5-Nse2 (wild-type); grey triangles Arm/Smc5-Nse2 (K333E/K344E); green circles Arm/Smc5-Nse2 (K764E); pink triangles Arm/Smc5-Nse2 (K333E/K344E/K764E); red diamonds Arm/Smc5-Nse2 (K743E/K745E). **(B) Left**, tryptophan intrinsic fluorescence of wild-type Arm/Smc5-Nse2. Black line in each panel, native Arm/Smc5-Nse2 without bound DNA; blue line, 5kb circular ssDNA/Smc5-Nse2; pink line, 50nt linear ssDNA/Smc5-Nse2; and green line, 20nt linear ssDNA/Smc5-Nse2. **Right,** conformational changes of wild-type Arm/Smc5-Nse2 induced by different types of DNA quantified by changes in center of mass (CM, red shift) of fluorescence spectra upon titration of the ligand until signal change achieved saturation. Blue circles, 5kb circular ssDNA/Smc5-Nse2; pink diamonds and 50nt linear ssDNA/Smc5-Nse2. **Inset**, titration curves of 5kb circular ssDNA/Smc5-Nse2 reactions containing 0 or 100mM NaCl (solid and hollow symbols). **Below**, table of the dissociation constants of the curves. **(C)** Degree of conformational changes in CM induced by 60nt linear ssDNA. Blue bar, Arm/Smc5-Nse2 (wild-type); grey bar, Arm/Smc5-Nse2 (K333E/K344E); green bar, Arm/Smc5-Nse2 (K764E); pink bar, Arm/Smc5-Nse2 (K333E/K344E/K764E); red bar, Arm/Smc5-Nse2 (K743E/K745E). Reactions were performed at least in three different independent experiments. Data values are mean ± s.d. and n=3 technical replicates. Significance was measured by a two-tailed unpaired t-test relative to wild-type. ****$P < 0.0001$.

Figure 5. A positively charged patch in Smc5 is required for DNA repair in vivo. (A) Ribbon representation of the complex between the *ARM* domain of Smc5 (yellow and orange) and Nse2 (red) (PDB *3HTK*) (Duan *et al*, 2009), showing positions of mutated lysine residues covered with black asterisks (3KE: K743E,K745E,K764E; 4KE: K337E,K344E,K354E,K355E; and 7KE: K337E,K344E,K354E,K355E,K743E,K745E,K764E). **(B)** Growth test analysis of wild-type, *nse2-CH* and the indicated *smc5-KE* mutants; 10-fold serial dilutions of the liquid

cultures were spotted in YPD and pictures taken after 48 hours. **(C)** Same as in (B) but using the *nse2-CH*, *smc5-3KE, smc5-K743,745E, smc5-K743,745R, smc5-7KE and smc5-7KR* mutants.

Figure 6. A DNA sensor in Smc5 participates in sumoylation in vivo.
(A) Protein extracts from exponentially growing wild-type, *smc5-3KE*, *smc5-K743,745E*, *smc5-4KE* and *smc5-K743,745R* cells were prepared under denaturing conditions; 6xHis-Flag tagged SUMO (HF-SUMO) was pulled down from protein extracts to purify sumoylated species and analyzed by western blot. A strain with no HF-tag was used as control; arrow points to unmodified form of the protein, vertical bar to sumoylated forms. **(B) Left,** same as in (A), but using wild-type and two independent clones of *smc5-7KE*; **right**, same as in (A), but using wild-type, *smc5-7KE* and *smc5-7KR* mutant cells. **(C)** Quantification of Smc5 sumoylated species in pull downs from the indicated *smc5-KE* mutants, relative to wild-type controls from at least three independent experiments. Boxes, 25–75% data range; whiskers, total data range; black bar, median; grey cross, mean. ****$P < 0.0001$; ***$P<0.001$; **$P < 0.01$; *$P<0.05$. 1-way ANOVA, *n* = number of samples analyzed. **(D)** Co-immunoprecipitation analysis of the Smc5-Nse2 interactions. *NSE2-6HA* cells were transformed with centromeric plasmids expressing the indicated *SMC5* alleles, and protein extracts from exponentially growing cells subjected to anti-HA immunoprecipitation. A strain with no HA tag was used as control. **(E)** Same as in (D), but using *SMC6-6HA* cells. **(F)** Quantification of Smc5-6HA signal from immunofluorescence on chromosome spreads prepared from exponentially growing cultures of the indicated genotypes. The mean value on wild-type spreads was arbitrarily set to 1; each dot represents one nucleus; red line, median; n=number of nuclei analyzed. ****$P < 0.0001$.

Figure 7. Model for ssDNA-dependent activation of the SUMO E3 ligase Nse2. Smc5/6 complex first uses its ATPase activity to associate with DNA. After loading onto DNA, binding of the positively charged patch (DNA sensor) in the Smc5 ARM domain further activates the Nse2 SUMO ligase. Nse1, Nse3, Nse5 and Nse6 subunits of the Smc5/6 complex are not shown in the figure.

Figure legends EV

Figure EV1. Enhancement of the SUMO E3 ligase activity of Smc5-Nse2 upon binding to DNA.

A. Time course conjugation reaction of SUMO1(***left***) or Smt3 (***right***) in the presence or absence of ssDNA (virion ϕx174) at 8 nM using full-length Smc5-Nse2 complex. The substrate utilized was the C-terminal *kleisin* domain of Nse4 (*cNse4*). Reactions using human or yeast E1 and E2 enzymes, for SUMO1 and Smt3, respectively, were run at 30°C and stopped at indicated minutes by adding SDS-loading buffer. Labels indicate the bands in the SDS-PAGE of the proteins in the reaction mixture. (*N-S1, cNse4-SUMO1; N-2S1, cNse4-2SUMO; N-Smt3, cNse4-Smt3; N-2Smt3, cNse4-2Smt3*).

B. SYPRO-stained SDS-PAGE of one of the triplicate SUMO conjugation reactions used to calculate the ssDNA *vs* dsDNA plot in figure 1B. The reactions were run for 60 min at 30°C and stopped by adding SDS-loading buffer.

C. SYPRO-stained SDS-PAGE of one of the triplicate SUMO conjugation reactions used to calculate the oligonucleotide plot in figure 1C. The reactions were run for 60 min at 30°C and stopped by adding SDS-loading buffer.

Figure EV2. Mutagenesis analysis of the SUMO E3 ligase activity of the Smc5-Nse2 constructs upon binding to DNA.

A. SYPRO-stained (*left*) and western-blot (*right*) of the time course reaction of SUMO conjugation in the presence or absence of ssDNA (virion ϕx174) at 8nM, using either wild-type *Arm/Smc5-Nse2* or K337E/K344E/K764E mutant. The reactions were run at 30°C with in the presence of the C-terminal *kleisin* domain of Nse4 as a substrate. (*N-S2, Nse4-SUMO2; N-2S2, Nse4-2SUMO2; N-3S2, Nse4-3SUMO2 and pS2, poly-SUMO2*).

B. SYPRO-stained SDS-PAGE of SUMO conjugation reactions of wild-type *Arm/Smc5-Nse2* at indicated NaCl concentrations in the presence or absence of ssDNA (virion ϕx174) at 8nM. (*N-S2, Nse4-SUMO2; N-2S2, Nse4-2SUMO2; N-3S2, Nse4-3SUMO2 and pS2, poly-SUMO2*).

C. SYPRO-stained SDS-PAGE of SUMO conjugation reactions of wild-type and 7KE mutant of Δhinge/*Smc5-Nse2 and* Δhead/*Smc5-Nse2* in the presence or absence of 50nt ssDNA.

Figure EV3. Conformational changes in Arm/Smc5-Nse2 followed by tryptophan intrinsic fluorescence (raw data).

A. Ribbon representation of the complex between the *ARM* domain of Smc5 (yellow and orange) and Nse2 (magenta) (PDB 3HTK). Tryptophan residues in Nse2 are labeled and shown in stick representation (blue). Zinc atom in the Nse2 RING domain is depicted as a yellow sphere.
B. Intrinsic Trp-emission spectra of wild-type *Arm/Smc5-Nse2***;** K333E/K344E**;** K764E**;** K333E/K344E/K764E; and K743E/K745E mutants. Colored thick lines, native Arm/Smc5-Nse2 without bound ligand (no 60nt linear ssDNA); black lines, emission spectra after addition of DNA in a concentration able to induce the half of the maximal transition determined by titration experiments.
C. Values of center of mass before and after DNA addition. These data were used to calculate the ΔCM presented in Fig 4C.

Figure EV4. Enhancement of the SUMO E3 ligase activity of Smc5-Nse2 upon binding to enoxaparin.

A. Time-course of the SUMO2 conjugation in the presence of increased concentration of enoxaparin using recombinant full-length/ or ARM/Smc5-Nse2 complex. The substrate utilized was the C-terminal *kleisin* domain of Nse4 (*cNse4*). Reaction was run at 30°C and stopped at indicated minutes by adding SDS-loading buffer. Φ stands for the 5kb virion ssDNA (5nM) used as positive control. Labels indicate the bands in the SDS-PAGE of the proteins in the reaction mixture. N-S2, cNse4-SUMO2; N-2S2 and pS2, polySUMOylation.
B. Western-blot of the samples presented in panel A. SUMOylated proteins were immunodetected by an anti-SUMO2 antibody

Figure EV5. Counter-charge mutation in various lysine residues of the positively charge patch in Smc5 lead to increased MMS sensitivity.

Growth test analysis of yeast strains carrying an endogenous *SMC5* gene under the *GAL* promoter. Each strain expresses the indicated *SMC5* allele form a centromeric plasmid; 10-fold serial dilutions of the liquid cultures were spotted in solid media containing the indicated concentration of MMS, and pictures taken after 48 hours.

METHODS

DNA substrates

Oligonucleotides sequences were randomly selected: 20nt (ATGGAGGTGGATGCAGCAGTA), 34nt (GACAGGATCCATGTCTAGTACAGTAATATCAAGG), 50nt (TGCCATATTGACAAGACGGCAAAGATGTCCTAGCAATCCATTGGTGATCA) and 60nt (CGCGGTCGACGGTTACCCATACGATGTTCCTGACTATGCGGCCTTGAACGATAATCCTAT). Circular single-strand DNA, ΦX174 (5kb), was purchased from New England Biolabs. pET28a (5kbp) and pETDUET-1 (5kbp) circular double-stranded DNA were purchased from Novagen.

Plasmids construction for overexpression in bacterial cells

For biochemical assays, open reading frame of full-length *SMC5* from *Saccharomyces cerevisiae* S288c was cloned into pET28a vector. COIL/PCOILS (Alva *et al*, 2016) was used to predict the boundaries of Smc5 *Head*, *Arm* and *Hinge* domains. The three constructs generated by PCR amplification *ΔHinge/SMC5* (Met1-Thr366 and Arg737-Asp1093 linked by a two-amino-acid linker peptide Gly-Thr), *ΔHead/SMC5* (Lys310-Glu815), and *Arm/SMC5* (Asp302-Thr366-Gly-Thr-Arg737-Gln813) were then individually cloned into pET28a vector. By the use of the mutagenesis protocol, the following mutations were introduced into *Arm-SMC5* expression vector: (K333E), (K344E), (K757E), (K764E), (K770E), (K777E), (K337E/K344E), (K743E/K745E), (K337E/K344E/K764E) and (K743R/K745R). We also introduced 7KE (K337E/K344E/K354E/K355E/K743E/K745E/K764E) mutations into *ΔHinge/* and *ΔHead/SMC5*. To allow co-expression with *SMC5* constructs, the ORF of full-length budding yeast *NSE2(MMS21)* was cloned into pET15b vector.

Protein expression and purification

All Full-length/, ΔHinge/, ΔHead/, and Arm/Smc5 recombinant proteins containing N-terminal His6-tag were co-expressed with His6-tag-Nse2 in *Escherichia coli* Rosetta 2(DE3) cells (Novagen). Alternatively, His6-tag-Nse2 was expressed alone using the same cell system. Bacterial cultures were grown at 37°C to OD_{600}=0.6, before 0.5 M IPTG addition. Cultures were then incubated for 4h at 30°C (Full-length /Scm5-Nse2, and Nse2) or for 16h at 20°C (ΔHinge/, ΔHead/, and Arm/Scm5-Nse2 wild-type and mutants) and harvested by centrifugation.

Cell pellets were equilibrated in Lysis Buffer (20% sucrose, 50 mM Tris pH 8.0, 1 mM

2-mercaptoethanol, 350 mM NaCl, 20 mM Imidazole, 0.1% IGEPAL), and cells were disrupted by sonication. Cell debris was removed by centrifugation (40,000×g). Hexa-histidine tagged proteins were purified by metal affinity chromatography using Chelating Sepharose Fast Flow resin (GE Healthcare) and eluted with 20 mM Tris pH 8.0, 350 mM NaCl, 1 mM 2-mercaptoethanol, and 250 mM imidazole. Fractions containing the Nse2, Full-length/Smc5-Nse2, ΔHinge-Smc5, ΔHead-Smc5, or Arm/Smc5-Nse2 (wild-type and mutants) were further purified by gel filtration (Superdex 200 HiLoad; GE Healthcare) followed by ion-exchange chromatography (Resource Q, or S for ΔHead-Smc5; GE Healthcare).

Smc5-Nse2 SUMOylation reactions

SUMOylation reactions of Nse2 (monomer), or Full-length/, ΔHinge/, ΔHead/, and Arm/Smc5-Nse2 (heterodimers) were performed in a reaction mix containing 40 mM HEPES (pH 7.5), 10 mM $MgCl_2$, 0.2% Tween 20, 50 mM NaCl, 4 mM dithiothreitol, 2 mM ATP, 32 µM SUMO1 or 2, 2 µM cNse4 (C-terminal *kleisin* domain, Ile246-Asp402), 300 nM Sae1-Sae2 (E1), 200 nM Ubc9 (E2) and the E3 (0.8 µM Nse2 alone, 0.38 µM Full-length/Smc5-Nse2, 0.48 ΔHead/Smc5-Nse2, 0.42 µM ΔHinge/Smc5-Nse2, or 1.25 µM Arm/Smc5-Nse2). The same reactions were also performed in parallel with the addition of DNA substrates (5kb circular ssDNA, 5kb circular dsDNA,-, 60nt-, 50nt-, 34nt- and 20nt--oligonucleotides) or enoxaparin at indicated concentrations. Samples were taken in different time intervals and stopped with SDS-Sample loading buffer (0.25 M Tris-HCl buffer pH 6.8, 10% (w/v) SDS, 30% (v/v) Glycerol, 0.7 M 2-Mercaptoethanol, and 0.05% Bromophenol blue). For dose-dependent experiments, increased DNA amounts (see Figure1) were added to reaction tubes and aliquots were taken after 60 minutes and stopped with SDS-Sample loading buffer. Products were verified by SDS-PAGE and visualized after SYPRO Ruby (Invitrogen) staining or by Western blotting with anti-SUMO1 or anti-SUMO2 (Sigma-Aldrich), or anti-T7 (Novagen). Single turnover experiment was performed as described (Yunus & Lima, 2005) with minor changes. The E2-thioester was formed in a reaction mix that includes 20 mM HEPES (pH 7.5), 50 mM NaCl, 10 mM $MgCl_2$, 0.1% Tween 20, 400 nM DTT, 100 nM Sae1-Sae2 (E1), 1 µM Ubc9 (E2) and 500 nM of (Alexa488)-labeled SUMO1. The reaction was initiated by the addition of 1 µM ATP and was incubated at 30°C for up to 15 min. Then, the reaction was quenched with the addition of 5 mM EDTA. To follow the thioester transfer mediated by the E3, we added to the reactions 1.25 µM Arm/Smc5-Nse2 (E3) and 2 µM of cNse4 (substrate) in the absence or presence of 0.8 µM of 50nt-oligonucleotide. Products of the time-course reactions were analyzed by SDS-PAGE and visualized by Alexa488 fluorescence emission in a Molecular Imager

Versadoc MP4000 System (Bio-Rad).

Electrophoretic mobility shift assay (EMSA)

Circular 5kb ssDNA template was used in EMSA reactions as provided by the supplier using a similar protocol reported by (Roy *et al*, 2011). For DNA-binding experiments, reaction mixtures contained 10 mM HEPES pH 7.5, DNA substrate (200 ng, 10 nM), and Arm/Smc5-Nse2 (wild-type or mutants) or kleisin domain of Nse4 (cNse4) in a 0- to 4,000-fold molar excess over DNA; see figure legends for Arm/Smc5-Nse2-to-DNA molar ratios. After incubation at 30°C for 40 min, the reactions were stopped by addition of an equal volume of 1.6% low melting point (LMP) agarose containing loading buffer (0.6% glycerol, 0.005% bromophenol blue final concentrations). Mixtures were loaded on 0.5% agarose-TAE gels and the DNA was resolved by electrophoresis at 2.5 V/cm for 19 h at 4°C. DNA bands were visualized after staining the gel with GelRed (Biotium) and documented by Gel Doc XR System (Bio-Rad). The experiments were performed in triplicate.

Spectroscopic Measurements

Circular dichroism (CD) measurements were performed using a Jasco-715 spectropolarimeter. Arm/Smc5-Nse2 (wild-type and mutants) were diluted in 4 mM HEPES pH 7.5 buffer to a final concentration of 3 µM. Circular 5kb ssDNA was titrated at various ratios and the contribution of buffer and DNA to the spectra was subtracted for background correction. Spectra were recorded as an average of ten scan accumulations with a scan rate of 200 nm/min, with 0.1 nm steps in a 1-mm path length cuvette at 30°C. Raw data were converted to mean residue ellipticity.

Intrinsic fluorescence spectra were recorded using a Jasco FP-8200 spectrofluorimeter. Tryptophan emission spectra were obtained by setting the excitation wavelength at 295 nm and collecting emission in the 310–400 nm range. These spectra were quantified as the center of spectral mass (v) according to equation: $v = \Sigma v_i F_i / \Sigma F_i$ where F_i stands for the fluorescence emission at a given wavelength (v_i) and the summation is carried out over the range of appreciable values of F (Foguel & Silva, 1994; Silva *et al*, 1986). Arm/Smc5-Nse2 (wild-type and mutants) were diluted to achieve 1 µM in 20 mM HEPES pH 7.5 buffer containing 0 or 0.1 M NaCl. In the titration experiments, circlular ssDNA (5kb) was tittered up to 5 nM, and the linear ssDNA (50nt) was tittered up to 5 µM. In the measurements with Arm/Smc5-Nse2 mutants, a linear ssDNA (60nt) was added to the reaction mixture to a final concentration of 0.2 µM in 20 mM HEPES pH 7.5 buffer. The temperature was

maintained at 30°C. Kd were calculated with GraphPad Prism4 using ligand binding mode with triplicates (Motulsky & Christopoulos, 2003).

Yeast growth test analysis

YTR31 cells (*MATa his3200 leu20 met150 trp63 ura30 GAL-3HA-SMC5:KAN bar1::URAca*), carrying the indicated *SMC5* alleles expressed from a centromeric plasmid, were inoculated in minimal dropout media containing galactose at 25ºC from freshly streaked plates until the culture reached exponential phase. In **Fig 5**, derivates from YPM2620 (*MATa his3Δ1 leu2Δ0 met15Δ0 ura3Δ0 6xHis-FLAG-smt3::kanMX6*) were grown to exponential phase in YPD. 10-fold serial dilutions from a culture at OD_{600}=0.5 were spotted as 3 µl drops onto YPD solid media and incubated at 30ºC for 2 days. As indicated, plates were supplemented with the indicated concentrations of methyl methanesulfonate (MMS).

SUMO pull down

Pull down analysis of sumoylated proteins was performed essentially as described (Colomina *et al*, 2017). To purify sumoylated proteins, the budding yeast SUMO gene (*SMT3)* was tagged N-terminally with a 6xHis-Flag epitope. 100 ODs cultures were collected and cells were mechanically broken in 6M guanidine chloride. Protein extracts were incubated with Ni-NTA beads in the presence of 15 mM imidazole overnight at room temperature. Beads were extensively washed with 8 M urea and bound proteins were eluted with SDS-PAGE loading buffer. Antibodies used in western blot analysis are anti-HA (3F10; Roche). To integrate the KE alleles into the genome, we fused an *SMC5* sequence containing the desired *smc5-KE* mutation to a 6HA-NAT selection marker. Clones were screened by anti-HA western blot and the presence of the KE mutations were confirmed by sequencing.

Immunoprecipitation and western blotting

For co-immunoprecipitation analysis, protein extracts from a 100 OD exponentially growing culture were prepared in EBX as previously described (Almedawar *et al*, 2012). HA-tagged proteins were immunoprecipitated using anti-HA Affinity matrix (Roche).

Detection of Smc5 on chromosome spreads by immunofluorescence

Exponentially growing cultures (5 ODs) were spheroplasted as previously described Grubb et al J Vis Exp (2015). After spheroplasting, 5 µl of gently resuspended spheroplasts were pipetted onto a glass slide before sequential addition of 10 µl

fixative (3.4% sucrose, 4% paraformaldehyde) and 20 µl of 2% lipsol as detergent. One minute later, 20 µl of fixative was added again in a swirling motion. A pipette tip on its side was used to gently spread the nuclei and chromosome spreads were air-dried overnight. For immunostaining, spreads were washed with PBS for 10 min in coplin jars and incubated with blocking solution (PBS, 2% milk, 5% BSA). Antibodies were incubated in blocking solution for 1 hour in a humidity chamber; monoclonal rat anti-HA (3F10, Roche) was used at 1:500 dilution to detect Smc5-6HA, followed by a 1:1000 dilution of Alexa488 labeled anti-rat antibody. After air-drying, DAPI was added in mounting media. For fluorescence microscopy, series of z-focal plane images were collected with a DP30 monochrome camera mounted on an upright BX51 Olympus fluorescence microscope.

Analysis of SUMOylation Efficiencies

Reactions rates of SUMOylation of cNse4 were quantified with ImageJ 1.49v software using the built-in gel-analyzer function (Schneider *et al*, 2012). Briefly, relative band intensities (fraction of SUMOylated protein) were calculated using a graphical method that involves generating lane profile plots, manually delineating peaks of interest, and then integrating peak areas. The calculations were performed at least in three different independent experiments **(Fig AV1**). Data values are mean ± s.e.m; and n=3 technical replicates. Significance was measured by a two-tailed unpaired t-test relative to wild-type. **P*<0.05, ***P*<0.01, ****P*<0.001.

Analysis of Smc5-SUMO from pull downs

Bands corresponding to Smc5 sumoylated species were quantified with ImageLab (BioRad). Smc5-SUMO signals for each *smc5* mutation were made relative to the wild-type. Four, two and one independent clones were analyzed for *smc5-7KE*, *smc5-3KE* and *smc5-4KE*, respectively, in at least three independent experiments. Statistical significance was measure by one-way ANOVA as described in the figure legend. *P* values of statistical significance are represented as *****P* <0.0001, ****P* <0.001, ***P* <0.01, **P* <0.05.

Degree of Conformational Changes

∆MRE at 222nm (%) induced by 5kb circular ssDNA was quantified by ligand titration until signal change achieved saturation, which was assumed to displays 100% of change. Reactions for wild-type protein were performed in three different independent experiments and data values are mean ± s.d.

∆CM(%) of fluorescence in the presence of 60nt ssDNA was quantified by calculating the difference between the Center of Mass of the samples (wild-type and mutants) before and after addition of a DNA concentration able to induce half of transitions seen in titration experiments using wild-type protein ($D_{1/2}$=4nm). This value was considered as 100% of change. Reactions were performed in three different independent experiments. Data values are mean ± s.d. and n=3 technical replicates. Significance was measured by a two-tailed unpaired t-test relative to wild-type. ****P<0.0001.

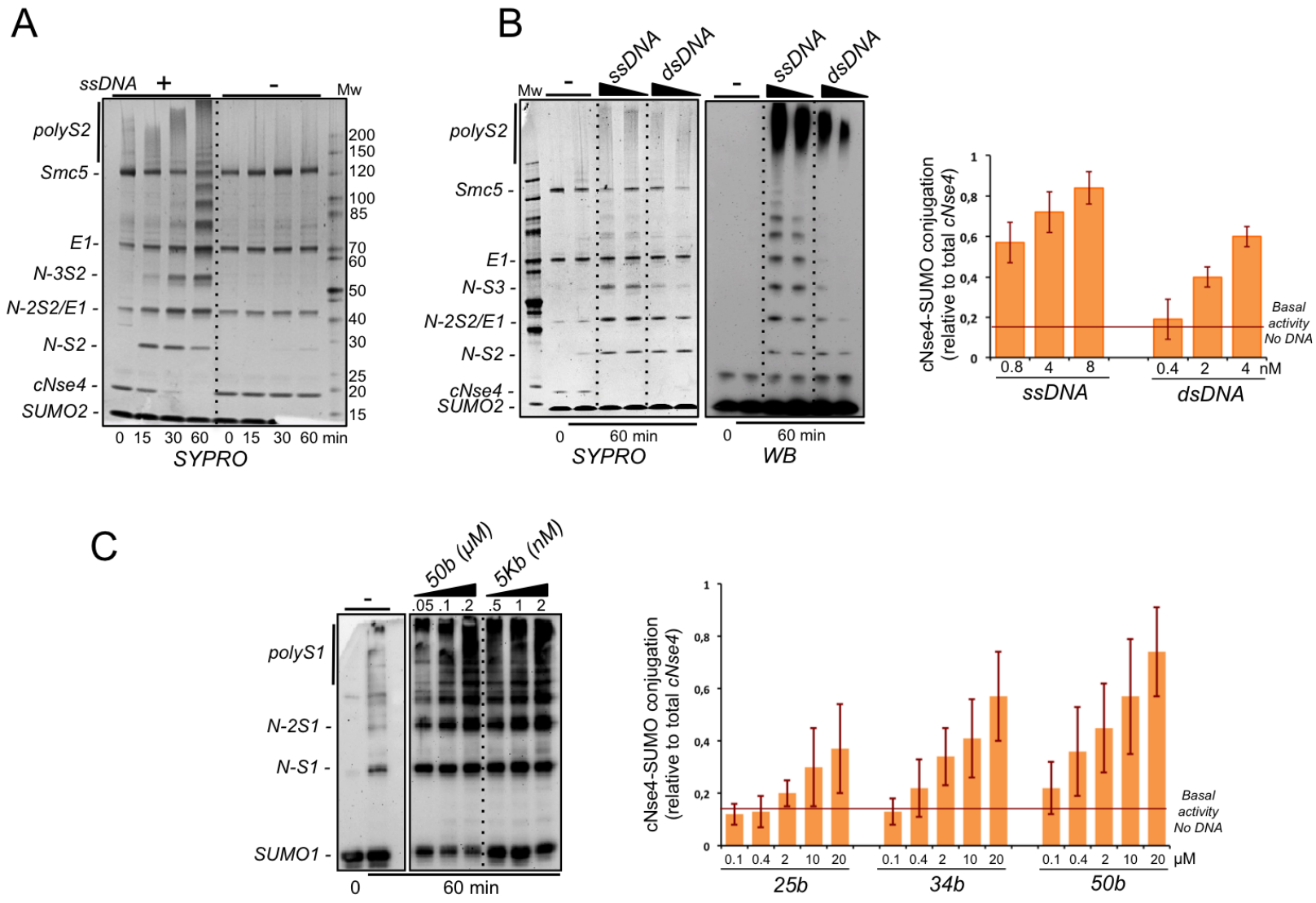
A
ssDNA
+
-
Mw
polyS2
Smc5 -
E1-
N-3S2 -
N-2S2/E1 -
N-S2 -
cNse4 -
SUMO2 -
200
150
120
100
85
70
60
50
40
30
25
20
15
0 15 30 60 0 15 30 60 min
SYPRO
B
Mw
-
ssDNA
dsDNA
-
ssDNA
dsDNA
polyS2
Smc5 -
E1-
N-S3 -
N-2S2/E1 -
N-S2 -
cNse4 -
SUMO2 -
0
60 min
SYPRO
0
60 min
WB
cNse4-SUMO conjugation
(relative to total cNse4)
1
0,8
0,6
0,4
0,2
0
Basal
activity
No DNA
0.8 4 8
0.4 2 4 nM
ssDNA
dsDNA
C
-
50b (μM)
.05 .1 .2
5Kb (nM)
.5 1 2
polyS1
N-2S1 -
N-S1 -
SUMO1 -
0
60 min
cNse4-SUMO conjugation
(relative to total cNse4)
1
0,8
0,6
0,4
0,2
0
Basal
activity
No DNA
0.1 0.4 2 10 20
0.1 0.4 2 10 20
0.1 0.4 2 10 20
μM
25b
34b
50b

Figure 1

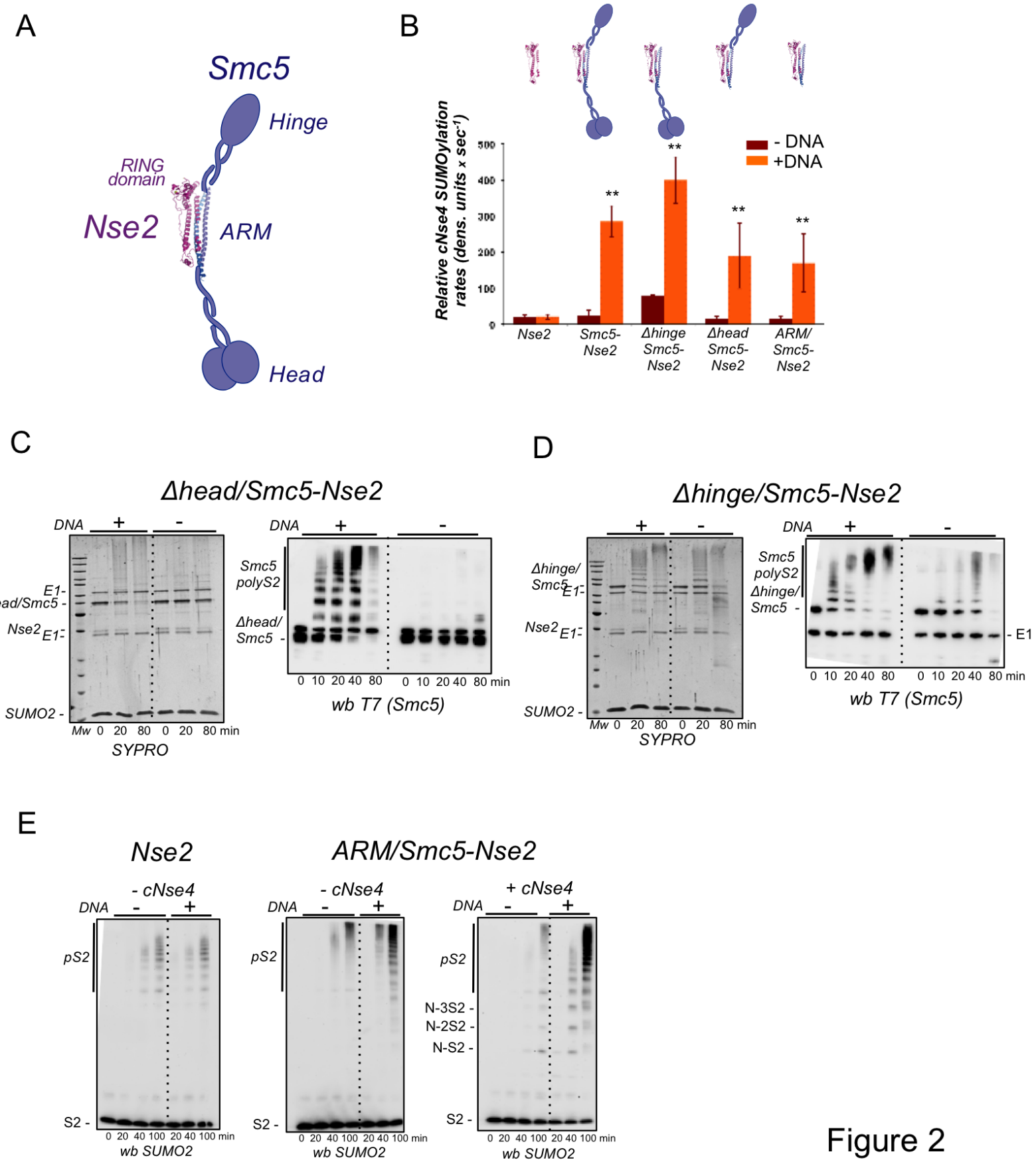
A
Smc5
Hinge
RING domain
Nse2
ARM
Head
B
Relative cNse4 SUMOylation rates (dens. units x sec-1)
- DNA
+DNA
**
Nse2
Smc5-Nse2
Δhinge Smc5-Nse2
Δhead Smc5-Nse2
ARM/ Smc5-Nse2
C
Δhead/Smc5-Nse2
DNA
E1-
Δhead/Smc5 -
Nse2 E1-
SUMO2 -
Mw 0 20 80 0 20 80 min
SYPRO
Smc5 polyS2
Δhead/ Smc5 -
0 10 20 40 80 0 10 20 40 80 min
wb T7 (Smc5)
D
Δhinge/Smc5-Nse2
Δhinge/ Smc5 E1-
Nse2 E1-
SUMO2 -
Mw 0 20 80 0 20 80 min
SYPRO
Smc5 polyS2
Δhinge/ Smc5 -
- E1
0 10 20 40 80 0 10 20 40 80 min
wb T7 (Smc5)
E
Nse2
ARM/Smc5-Nse2
- cNse4
+ cNse4
DNA
pS2
S2 -
N-3S2 -
N-2S2 -
N-S2 -
0 20 40 100 20 40 100 min
wb SUMO2

Figure 2

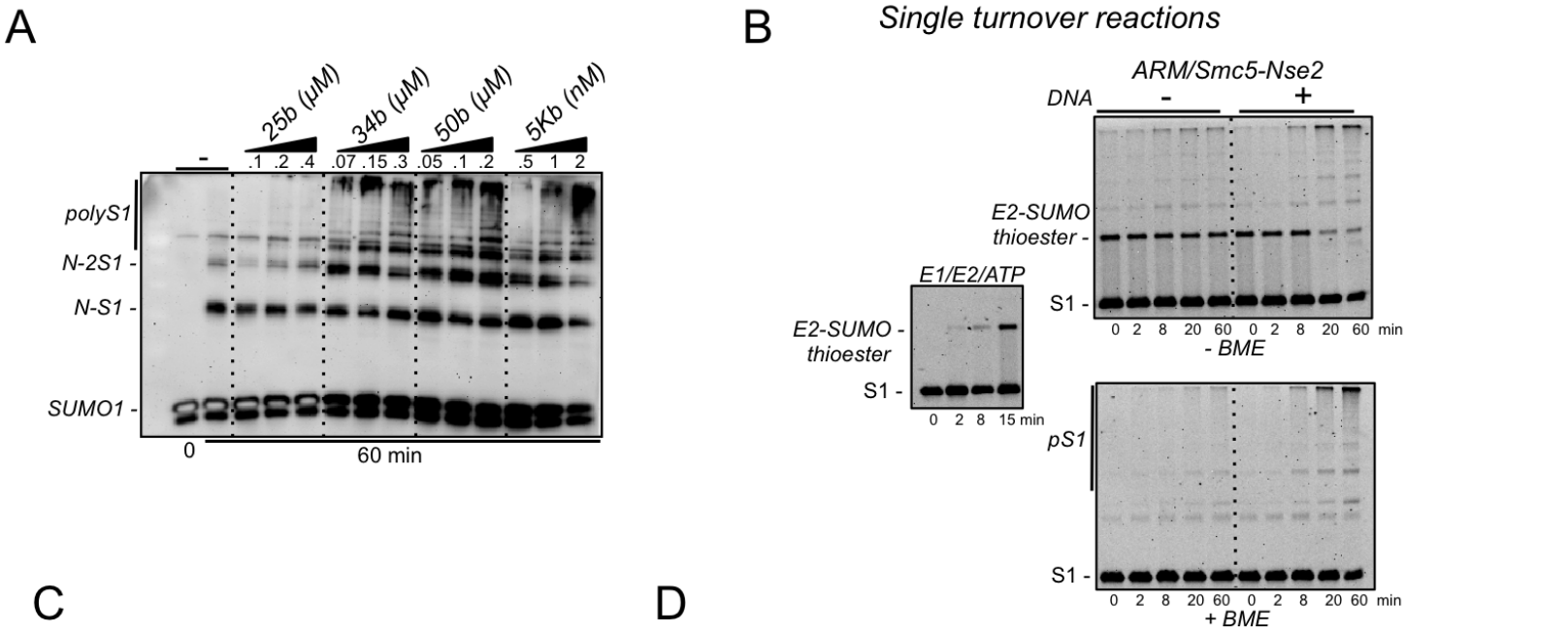
A
25b (μM)
34b (μM)
50b (μM)
5Kb (nM)
polyS1
N-2S1
N-S1
SUMO1
0
60 min
B
Single turnover reactions
ARM/Smc5-Nse2
DNA
E2-SUMO thioester
E1/E2/ATP
S1
- BME
pS1
+ BME
C
RING domain
Nse2
Arm/Smc5
D
cNse4 SUMO conjugation rate (relative to WT)
- DNA
+DNA
WT
K333E
K344E
K337E K344E
K337E K344E K764E
K743E K745E
K757E
K764E
K770E
K777E
K743R K745R
E
WT
K337E/ K344E/ K764E
K743E/ K745E
Φx174

Figure 3

A

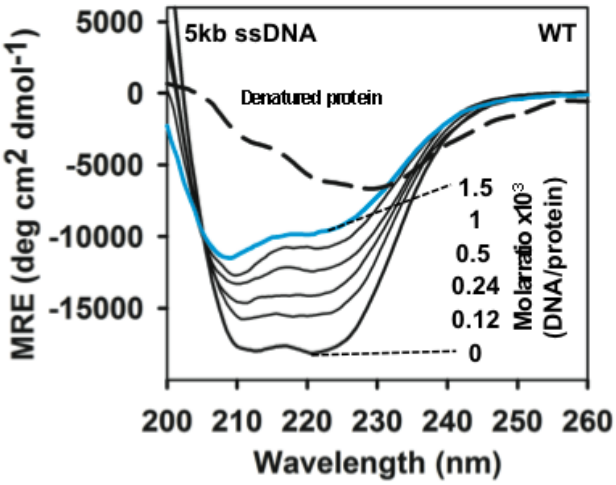

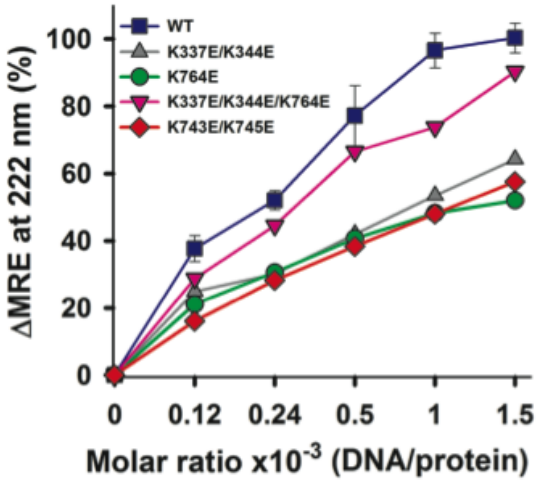

B

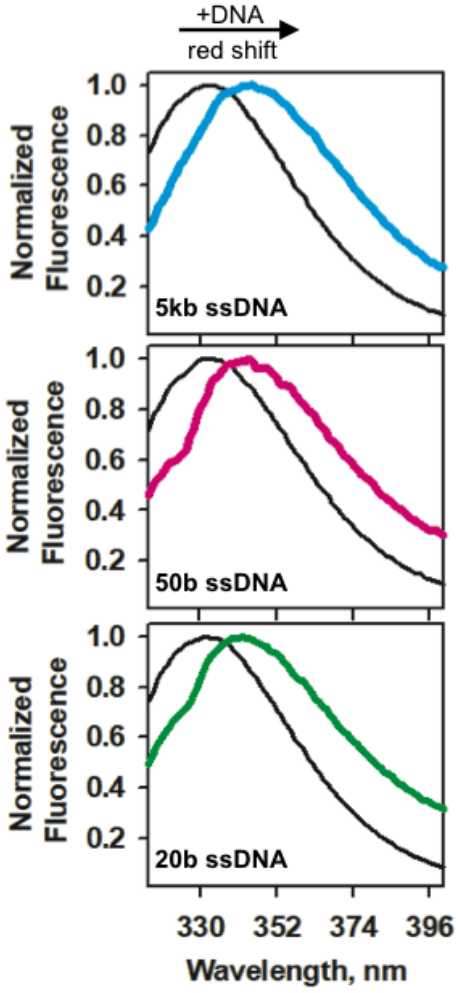

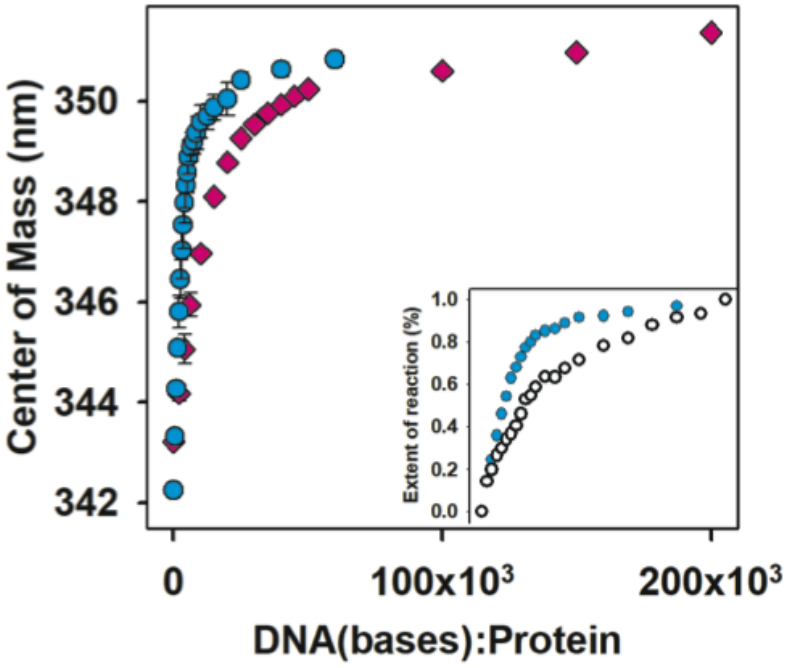

	K_d (nM)	Fold increment /bases
5kb ssDNA	0.70 ± 0.1	1
5kb ssDNA+NaCl	1.25 ± 0.7	1.7
50b ssDNA	190 ± 0.1	2.7

C

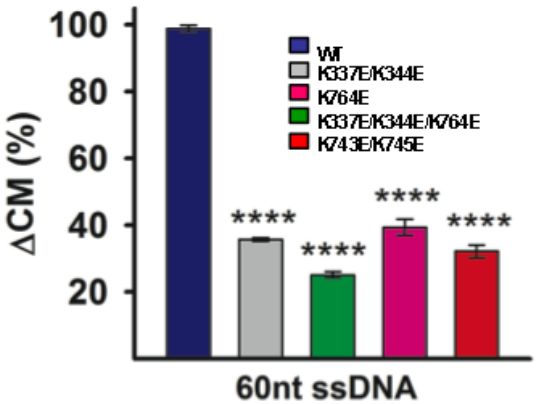

Figure 4

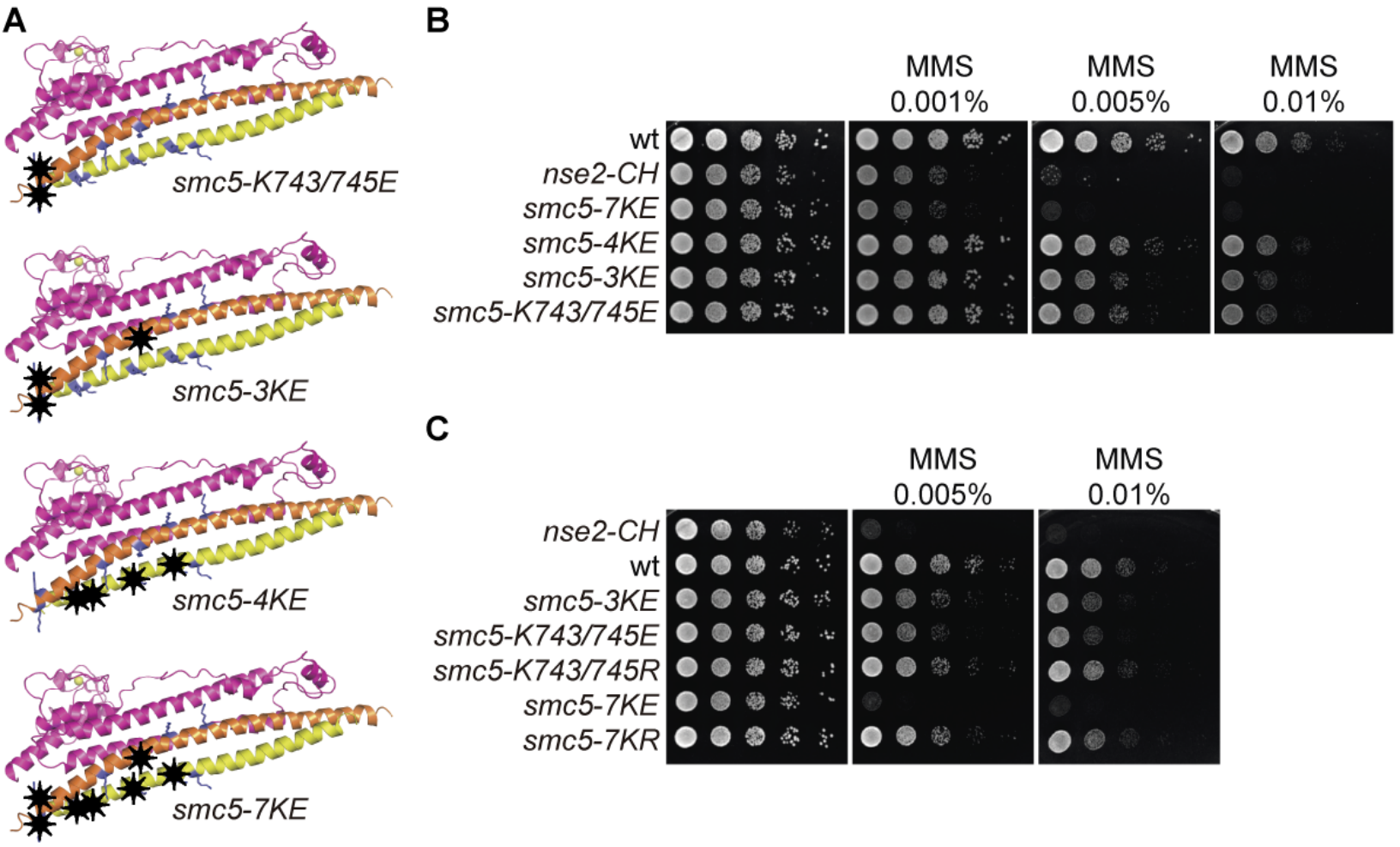
A
smc5-K743/745E
smc5-3KE
smc5-4KE
smc5-7KE
B
MMS
0.001%
MMS
0.005%
MMS
0.01%
wt
nse2-CH
smc5-7KE
smc5-4KE
smc5-3KE
smc5-K743/745E
C
MMS
0.005%
MMS
0.01%
nse2-CH
wt
smc5-3KE
smc5-K743/745E
smc5-K743/745R
smc5-7KE
smc5-7KR

Figure 5

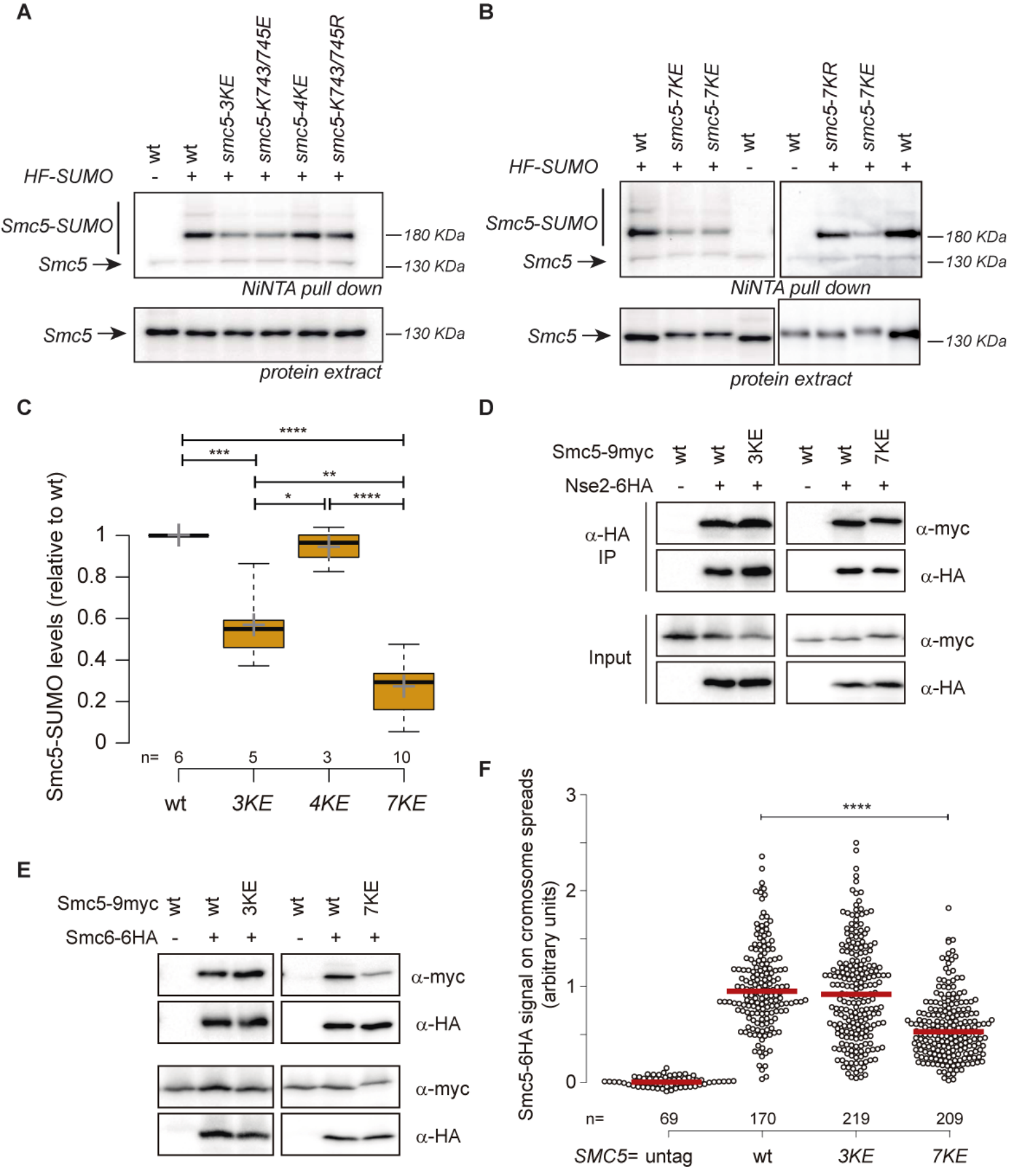
A
HF-SUMO
wt
wt
smc5-3KE
smc5-K743/745E
smc5-4KE
smc5-K743/745R
Smc5-SUMO
Smc5
180 KDa
130 KDa
NiNTA pull down
Smc5
130 KDa
protein extract
B
HF-SUMO
wt
smc5-7KE
smc5-7KE
wt
wt
smc5-7KR
smc5-7KE
wt
Smc5-SUMO
Smc5
180 KDa
130 KDa
NiNTA pull down
Smc5
130 KDa
protein extract
C
Smc5-SUMO levels (relative to wt)
n= 6 5 3 10
wt
3KE
4KE
7KE
D
Smc5-9myc
Nse2-6HA
wt
3KE
7KE
α-HA IP
α-myc
α-HA
Input
α-myc
α-HA
E
Smc5-9myc
Smc6-6HA
wt
3KE
7KE
α-myc
α-HA
α-myc
α-HA
F
Smc5-6HA signal on cromosome spreads (arbitrary units)
n= 69 170 219 209
SMC5= untag
wt
3KE
7KE

Figure 6

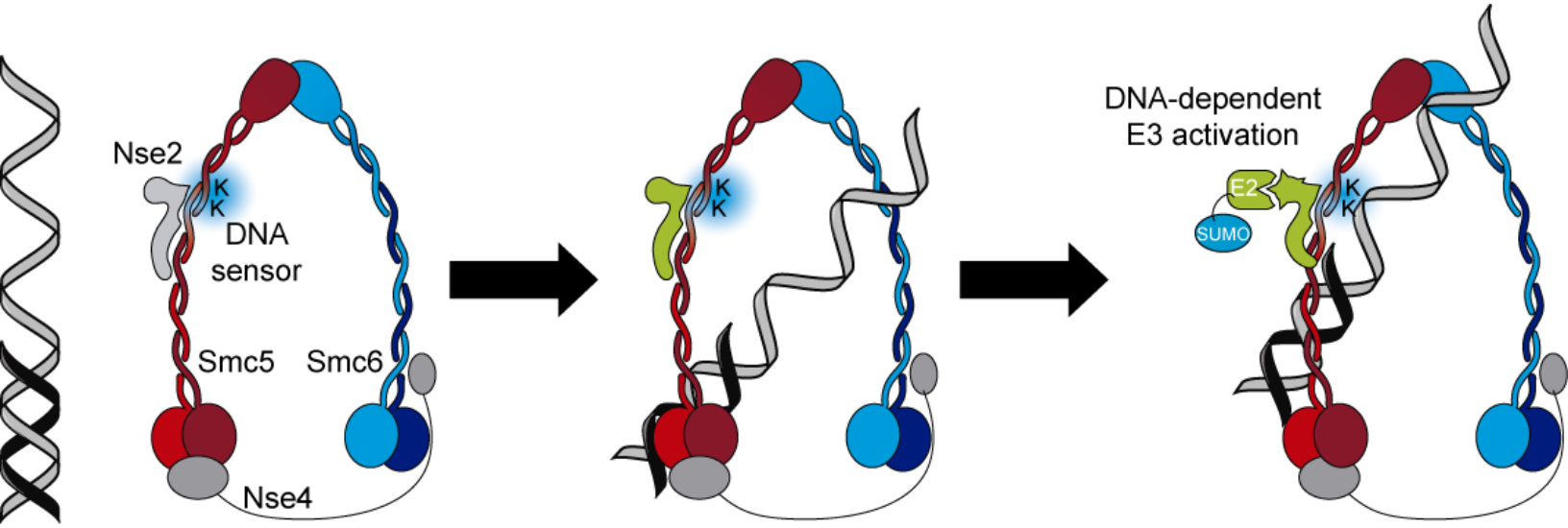
Nse2
K
K
DNA
sensor
Smc5
Smc6
Nse4
K
K
DNA-dependent
E3 activation
E2
SUMO
K
K

Figure 7

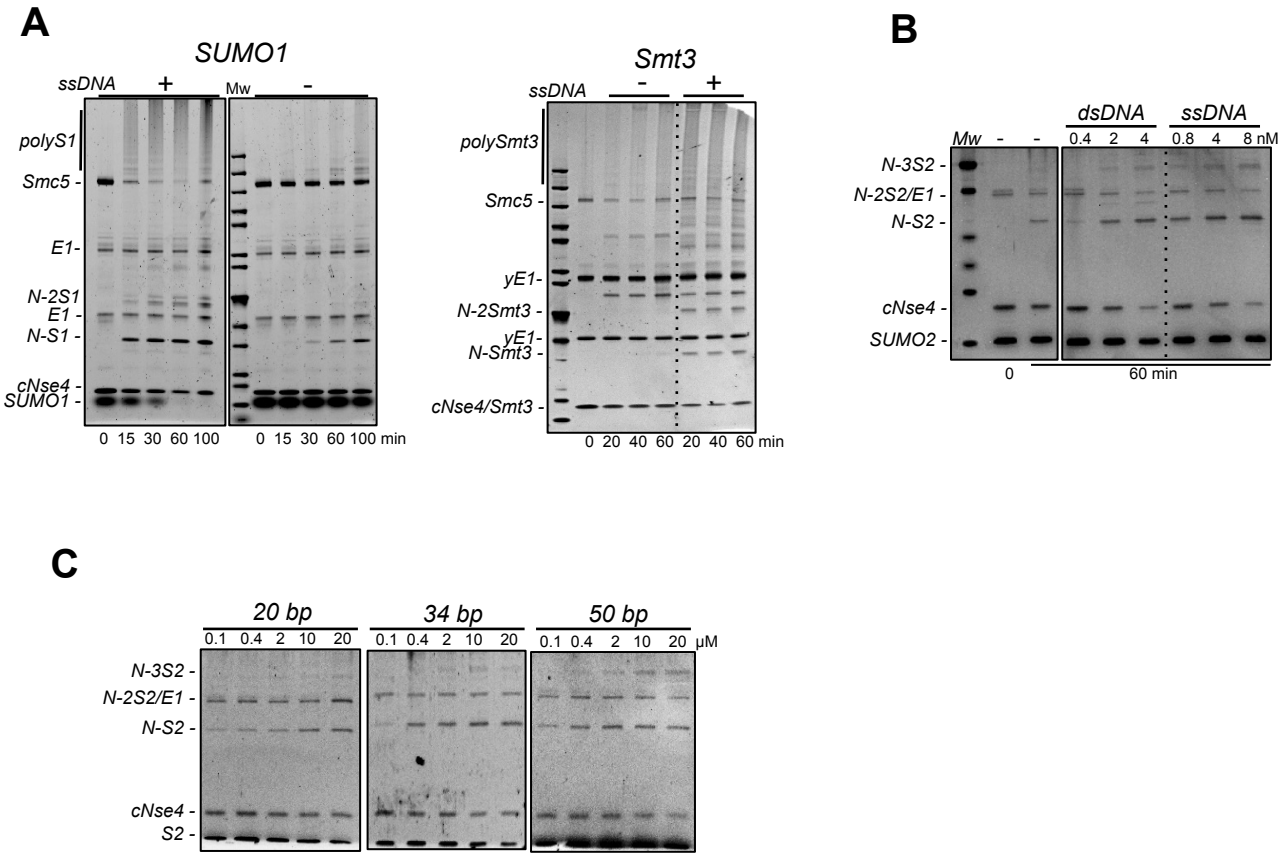
A
SUMO1
ssDNA
+
Mw
-
polyS1
Smc5 -
E1-
N-2S1
E1 -
N-S1 -
cNse4 -
SUMO1 -
0 15 30 60 100 0 15 30 60 100 min
Smt3
ssDNA
-
+
polySmt3
Smc5 -
yE1-
N-2Smt3 -
yE1-
N-Smt3 -
cNse4/Smt3 -
0 20 40 60 20 40 60 min
B
dsDNA
ssDNA
Mw
- -
0.4 2 4 0.8 4 8 nM
N-3S2 -
N-2S2/E1 -
N-S2 -
cNse4 -
SUMO2 -
0
60 min
C
20 bp
34 bp
50 bp
0.1 0.4 2 10 20 0.1 0.4 2 10 20 0.1 0.4 2 10 20 µM
N-3S2 -
N-2S2/E1 -
N-S2 -
cNse4 -
S2 -

Figure EV1

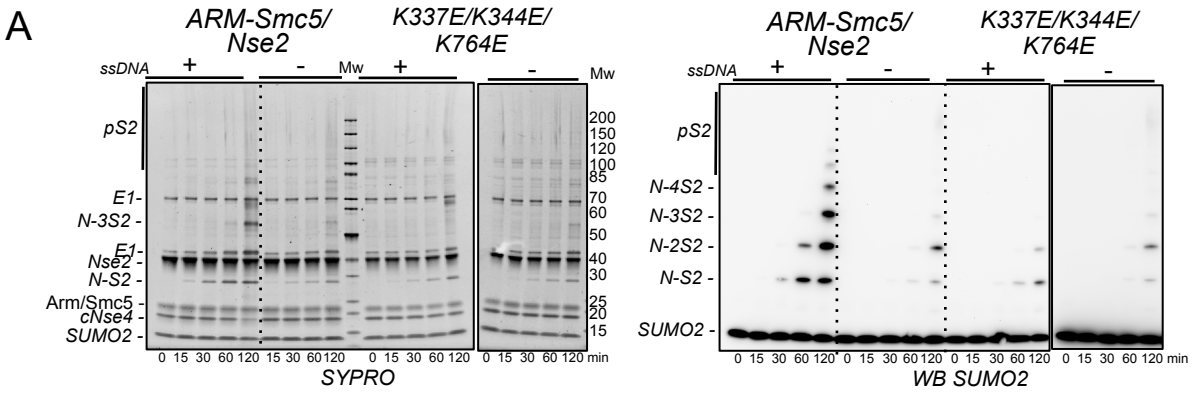
A
ARM-Smc5/ Nse2
K337E/K344E/ K764E
ssDNA
Mw
pS2
E1-
N-3S2 -
E1-
Nse2 -
N-S2 -
Arm/Smc5 -
cNse4 -
SUMO2 -
0 15 30 60 120 15 30 60 120 0 15 30 60 120 0 15 30 60 120 min
SYPRO
N-4S2 -
N-2S2 -
WB SUMO2

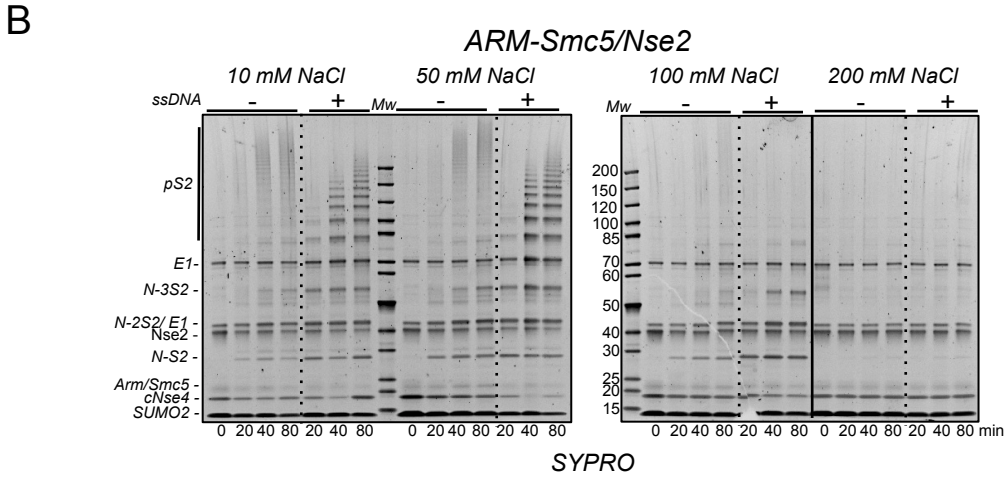
B
ARM-Smc5/Nse2
10 mM NaCl
50 mM NaCl
100 mM NaCl
200 mM NaCl
ssDNA
Mw
pS2
E1-
N-3S2
N-2S2/ E1 -
Nse2 -
N-S2 -
Arm/Smc5 -
cNse4 -
SUMO2 -
0 20 40 80 20 40 80 0 20 40 80 20 40 80 0 20 40 80 20 40 80 0 20 40 80 20 40 80 min
SYPRO

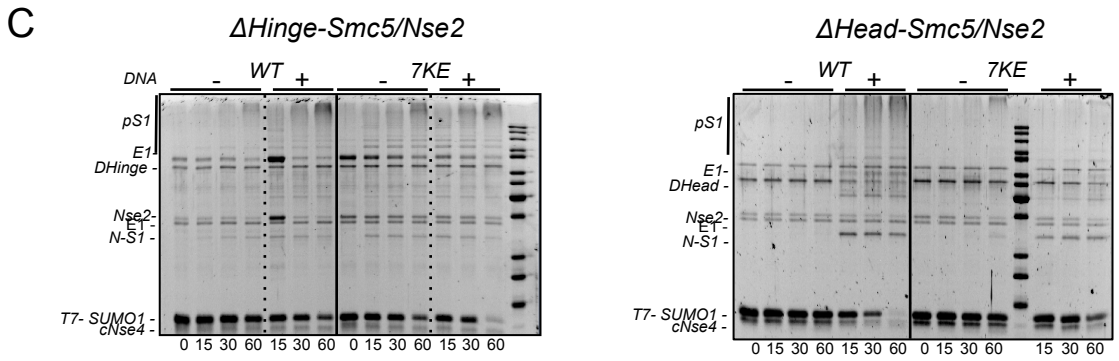
C
ΔHinge-Smc5/Nse2
ΔHead-Smc5/Nse2
DNA
WT
7KE
pS1
E1
DHinge -
DHead -
Nse2-
E1 -
N-S1 -
T7- SUMO1 -
cNse4 -
0 15 30 60 15 30 60 0 15 30 60 15 30 60
0 15 30 60 15 30 60 0 15 30 60 15 30 60

Figure EV2

A

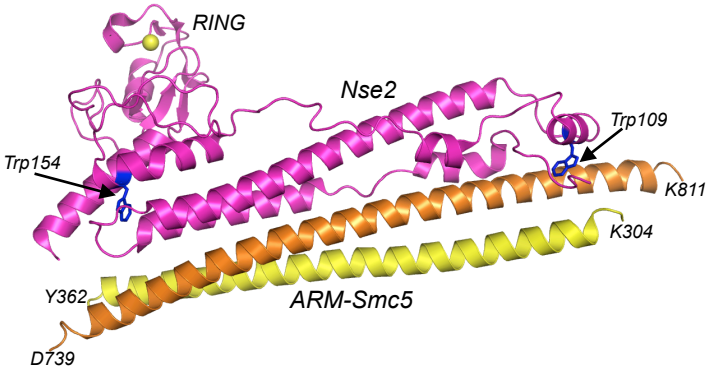

B

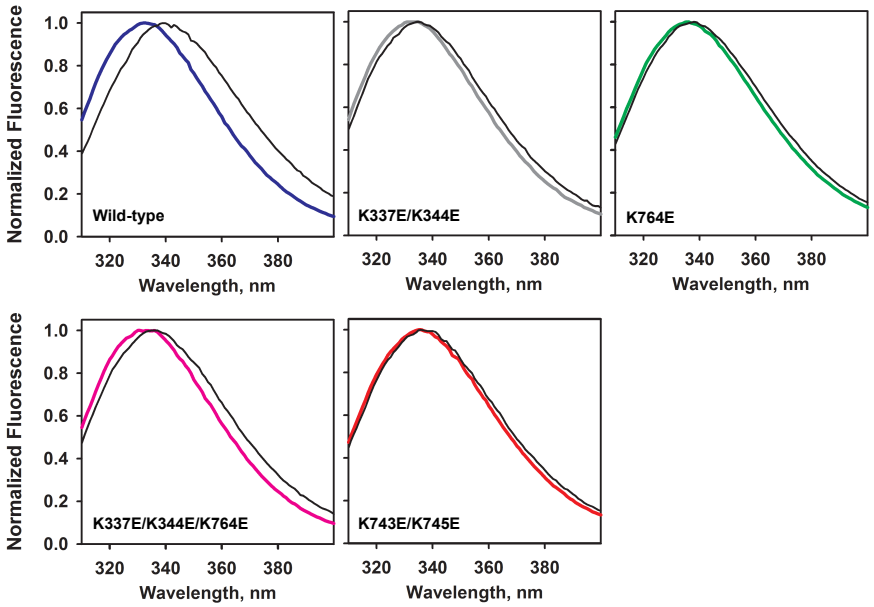

C

	Arm/Smc5 Nse2 (WT)	Arm/Smc5 Nse2 (K337E/K344E)	Arm/Smc5 Nse2 (K764E)	Arm/Smc5 Nse2 (K337E/K344E/K764E)	Arm/Smc5 Nse2 (K743/K745E)
Initial CM	341.9±0.02	342.2±0.17	344.2±0.07	343.1±0.14	343.7±0.10
Final CM	346.1±0.02	343.7±0.15	345.3±0.08	344.7±0.20	345.1±0.09
ΔCM	**4.2**	**1.5**	**1.1**	**1.6**	**1.4**

Figure EV3

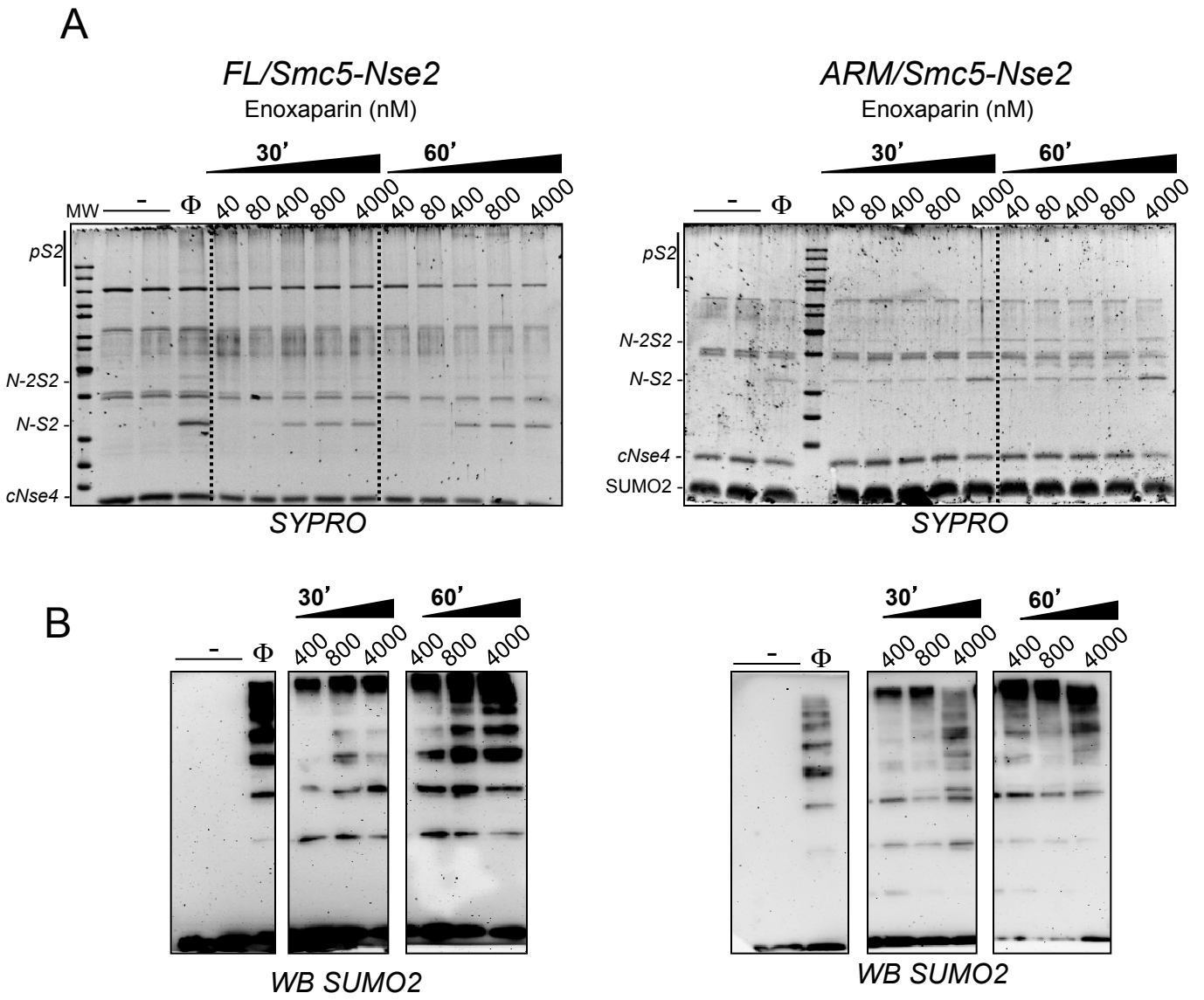
A
FL/Smc5-Nse2
Enoxaparin (nM)
30'
60'
MW
-
Φ
40
80
400
800
4000
pS2
N-2S2
N-S2
cNse4
SYPRO
ARM/Smc5-Nse2
Enoxaparin (nM)
SUMO2
B
WB SUMO2

Figure EV4

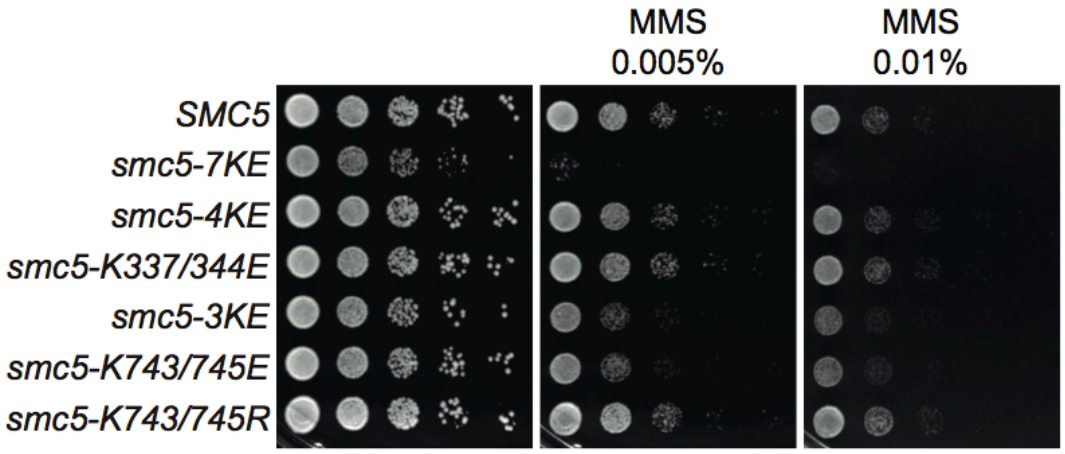
MMS
0.005%
MMS
0.01%
SMC5
smc5-7KE
smc5-4KE
smc5-K337/344E
smc5-3KE
smc5-K743/745E
smc5-K743/745R

Figure EV5